JOC *Article*

Gas-Phase Acidities of Disubstituted Methanes and of Enols of Carboxamides Substituted by Electron-Withdrawing Groups[1]

Masaaki Mishima,*,† Mio Matsuoka,† Yi Xiong Lei,‡ and Zvi Rappoport*,‡

Institute for Material Chemistry and Engineering, Kyushu University, 6-10-1 Hakozaki, Higashi-ku, Fukuoka 812-8581, Japan, and Department of Organic Chemistry and Minerva Center for Computational Quantum Chemistry, The Hebrew University, Jerusalem 91904, Israel

zr@vms.huji.ac.il

Received May 11, 2004

The gas-phase acidities ΔG°_{acid} of some 20 amides/enols of amides RNHCOCHYY′/RNHC(OH)═CYY′ [R = Ph, *i*-Pr; Y, Y′ = CO_2R', CO_2R'', or CN, CO_2R', R′, R″ = Me, CH_2CF_3, $CH(CF_3)_2$], the *N*-Ph and *N*-Pr-*i* amides of Meldrum's acid, 1,3-cyclopentanedione, dimedone, and 1,3-indanedione, and some *N*-*p*-BrC_6H_4 derivatives and of nine CH_2YY' (Y, Y′ = CN, CO_2R', CO_2R''), including the cyclic carbon acids listed above, were determined by ICR. The acidities were calculated at the B3LYP/6-31+G*//B3LYP/6-31+G* level for both the enol and the amide species or for the carbon acid and the enol on the CO in the CH_2YY' series. For 12 of the compounds, calculations were also conducted with the larger base sets 6-311+G* and G-311+G**. The ΔG°_{acid} values changed from 341.3 kcal/mol for $CH_2(CO_2Me)_2$ to 301.0 kcal/mol for PhNHC(OH)═C(CN)$CH(CF_3)_2$. The acidities increased for combinations of Y and Y′ based on the order $CO_2Me < CO_2CH_2CF_3 <$ CN, $CO_2CH(CF_3)_2$ for a single group and reflect the increased electron-withdrawal ability of Y,Y′ coupled with the ability to achieve planarity of the crowded anion. The acidities of corresponding YY′-substituted systems follow the order *N*-Ph enols > *N*-Pr-*i* enols ≫ CH_2YY'. Better linear relationships between ΔG°_{acid} values calculated for the enols and the observed values than those for the values calculated for the amides suggest that the ionization site is the enolic O−H of most of the noncyclic trisubstituted methanes. The experimental ΔG°_{acid} value for Meldrum's acid matches the recently reported calculated value. The calculated structures and natural charges of all species are given, and the changes occurring in them on ionization are discussed. Correlations between the ΔG°_{acid} values and the pK_{enol} values, which are linear for the trisubstituted methanes, excluding YY′ = $(CN)_2$ and nonlinear for the CH_2YY' systems, are discussed.

Data on enols (**2**) of carboxylic acid derivatives **1**[2] are slowly being gathered. These enols belong mainly to two groups: (i) short-lived enols of carboxylic acids **2**, X = OH, and (ii) enols of carboxylic acid amides, **2**, X = NHR.

Y′YCHC(=O)X **1**   Y′YC=C(OH)X **2**

For group i, which was mainly investigated by Kresge's group[2b,3] and less by others,[4] the main data measured include the equilibrium values (K_{enol} = [**2**]/[**1**]), the various rate coefficients involved in the carbonyl/enol/enolate transformation, and the acidities of the enol species in aqueous solution. These systems are not highly activated by electron-withdrawal from C_β. For group ii, several enols of carboxamides were observed as short-lived, either spectroscopically observable or detectable (e.g., by kinetics) or unobservable intermediates.[5] However, the majority of the systems known in which the enols are observable as long-lived species, either exclusively or in equilibria with the amides **1**, are mainly from our group, and the data on them include structural information such as crystallographic data and (*E*,*Z*)-geometry, K_{enol} values, and NMR data in aprotic solvents.[6]

These enols are substituted by two β-electron-withdrawing groups (EWGs) by resonance YY′. The rationale

---

† Kyushu University.

‡ The Hebrew University.

[1] Mishima, M.; Lei, X. Y.; Rappoport, Z. Presented in part at the 16th IUPAC Conference on Physical Organic Chemistry (ICPOC 16), University of California, San Diego, La Jolla, CA, Aug 4−9, 2002; Book of Abstracts, Abstract LC 21.

[2] For reviews, see: (a) Hegarty, F. A.; O'Neill, P. In *The Chemistry of Enols*; Rappoport, Z., Ed.; Wiley: Chichester, 1990; p 639. (b) Kresge, A. J. *Chem. Soc. Revs.* **1966**, *25*, 275.

[3] For early and late references to Kresge's work, see ref 2b and Bakulev V. A.; Chiang Y.; Kresge A. J.; Meng Q.; Morzherin Y. Y.; Popik, V. V. *J. Am. Chem. Soc.* **2001**, *123*, 2681.

[4] For example, see: Frey J.; Rappoport Z. *J. Am. Chem. Soc.* **1996**, *118*, 3994, 5169.

[5] (a) Rappoport, Z.; Frey, J.; Sigalov, M.; Rochlin, E. *Pure Appl. Chem.* **1997**, *69*, 1933. (b) Williams, D. H. L.; Xia, L. *J. Chem. Soc., Chem. Commun.* **1992**, 985; *J. Chem. Soc., Perkin Trans. 2* **1993**, 1429. (c) Chiang, Y.; Guo, H.-X.; Kresge, A. J.; Richard, J. P.; Toth, K. *J. Am. Chem. Soc.* **2003**, *125*, 187. (d) Wagner, B. D.; Arnold, B. R.; Brown, G. S.; Lusztyk, J. *J. Am. Chem. Soc.* **1998**, *120*, 1827. (e) Rapoet, G.; Nguyen, M. T.; Kelly, S.; Hegarty, A. F. *J. Org. Chem.* **1998**, *63*, 9669. (f) Kresge, A. J.; Meng, O. *Can. J. Chem.* **1999**, *77*, 1528. (g) Hegarty, A. F.; Eustance, S. J.; Relikan, C. 7th European Symposium on Organic Reactivity (ESOR7), Ulm, Germany, Aug 22−27, 1999; Abstract A8, p 68. (h) Hegarty, A. F.; Ryan M. 8th European Symposium on Organic Reactivity (ESOR8), Cavtat (Dubrovnik), Croatia, Sept 1−6, 2001; Abstract PA44, p 168. (i) Acton, O.; Allen, A. D.; Antunes, L, Fedovov, A.; Najufian, K.; Shang, M.; Tidwell, T. T.; Wagner, B. D. 16th IUPAC Conference on Physical Organic Chemistry, University of California, San Diego, La Jolla, CA, Aug 4−9, 2002; Abstract LA3.

10.1021/jo040196b CCC: $27.50

behind preparing such stable enols is shown in eq 1 and is demonstrated for X = NHR. Delocalization of the negative charge on the EWGs YY′ stabilizes the enol hybrid **2a**. The effect of YY′ on the amide species **1a** was assumed to be less important.

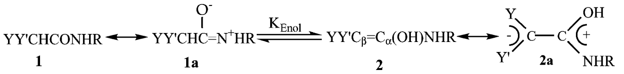

(1)

By using this approach, we obtained or observed more than 50 enols of carboxamides, many of them as the solid-state species and others in mixtures with the amides in solution.[6] The main activating groups used are CN and CO_2R, where R = CH_2CF_3, $CH(CF_3)_2$, or CH_2CCl_3. When Y,Y′ are lesser EWGs, e.g., Y = CO_2Me and Y′ = CO_2Me, $CO_2CH_2CF_3$, the species have the amide structure in the solid state. Many K_{enol} values were determined, and the reactions of the enols with diazomethane whose rates and products depend qualitatively on their acidities were investigated.[7]

Although data on acidities in solution of the enols investigated by Kresge are available,[2b,3] data on the acidities of both groups in the gas phase are not available, although mass spectrometric data on the enol cation radicals are known for a few systems.[8]

In the present work, we determined by an ICR technique the gas-phase acidities of 22 such enols/amides (including two with Y = Y′ = CO that enolize on the keto carbonyl) that differ in the N-substituent (Ph or *p*-BrC_6H_4 vs *i*-Pr) and in the combination of Y and Y′ as well as of nine corresponding carbon acids CH_2YY'.

The interest in these acidities is multifold. First, both the amides which are carbon acids, i.e., methanes trisubstituted by the EWGs Y,Y′ and CONHR, and the enols, which are vinylic oxygen acids, should be strong organic acids since the negative charge in the conjugate base should be delocalized on the oxygen, C_β, Y, and Y′. Consequently, the location of these carbon/oxygen acids on the acidity scale is interesting. Second, the meager data on the new functional group =C(OH)NHR will be enriched by such a study. Third, the equilibrium constant K_{enol}, which is an important parameter for enols, is related to the acidities of the amide A (K_a^A) and the enol E (K_a^E) species (eq 2) via a cycle that involves the common enolate intermediate. Hence, for calculating the gas-phase enol/amide equilibria ($\Delta G°_{AE} = -RT\ln K_{enol}$), the $\Delta G°_{acid}$ values of both the amide and the enol are required (eq 3).

$$K_{enol} = [E]/[A] = K_a^{\ A}/K_a^{\ E} \qquad (2)$$

$$\Delta G°_{AE} = \Delta G°_{acid}(E) - \Delta G°_{acid}(A) \qquad (3)$$

For stable simple enols $Ar_2C{=}C(OH)R$ of aldehydes and ketones $Ar_2CHC({=}O)R$, we had measured previously these values for the isolated species in several systems[9] and determined in this way the gas-phase K_{enol} values. This is not the case with enols of carboxamides where only one species is isolated for each system. However, the $\Delta G°_{AE}$ values can be calculated and compared with the experimental $\Delta G°_{acid}$ values in order to evaluate to what extent the similar role of the EWGs both in the stabilization of the conjugate base of the acid and in increasing the stability of the enol via the hybrid **2a** affect the $\Delta G°_{AE}$ values.

Fourth, since hydrogen bonding to the solvent is important in solution, the gas-phase acidities in the absence of a solvent can give information on this interaction.

Fifth, since in the subseries when Y and Y′ are ester groups the solid-state structure is changed from that of the amide to that of the enol, whereas the enolate ion structures are analogous in both cases, it is of interest to find out if a possible difference in the ionization of the neutral precursors is reflected in the $\Delta G°_{acid}$ values.

Results

Systems Investigated. The compounds investigated belong to five subgroups. (A) One subgroup consists of open-chain malonic acid derivatives CH_2YY' having no amide enolization site. The acidities when Y = Y′ = CN, COMe are known.[10] (B) Another group consists of their *N*-Ph and two *N*-C_6H_4Br-*p* amide/enol derivatives ArNHCOCHYY′/ArNHC(OH)=CYY′, and (C) a third subgroup consists of the analogous *N*-*i*-Pr derivatives. The less activated species in series B and C have an amide structure in the solid, whereas the other species have an enol structure. Other subgroups consist of (D) the cyclic CH_2YY' systems 1,3-indanedione (IND), dimedone (DIM), whose acidity is known,[10] and 1,3-cyclopentanedione (CPD) activated by two β-keto groups (i.e., Y, Y′ = CO) and their enol derivatives and (E) the cyclic ester Meldrum's acid (MA) and its *N*-Ph, *N*-C_6H_4-Br-*p*, and *N*-*i*-Pr derivatives.

Acidity Determination. The acidities were determined by the ICR technique, by measuring the equilibrium constants of the reversible proton-transfer reaction between the investigated compound and a reference acid of known acidity. Two such acids, with acidity bracketing the acidities of the compound investigated, were usually used, and the selected $\Delta G°_{acid}$ values are given in Table 1. Since for each series the acidity spans large differences, a group of reference acids have to be used for each series. The compounds investigated, the reference acids with their $\Delta G°_{acid}$ values, the $\Delta\Delta G°_{acid}$, and the selected $\Delta G°_{acid}$ values for our compounds are given in Table 1.

The experimental values (Table 2) display the following features. (a) In series A, the weaker acid is dimethyl

---

[6] (a) Mukhopadhyaya, J. K.; Sklenak, S.; Rappoport, Z. *J. Am. Chem. Soc.* **2000**, *122*, 1325. (b) Mukhopadhyaya, J. K.; Sklenak, S.; Rappoport, Z. *J. Org. Chem.* **2000**, *65*, 6856. (c) Lei, Y. X.; Cerioni, G.; Rappoport, Z. *J. Org. Chem.* **2001**, *66*, 8379. (d) Lei, Y. X.; Casarini, D.; Cerioni, G.; Rappoport, Z. *J. Org. Chem.* **2003,** *68*, 947. (e) Lei, Y. X.; Casarini, D.; Cerioni, G.; Rappoport, Z. *J. Phys. Org. Chem.* **2003,** *16*, 525. (f) Basheer, A.; Rappoport, Z. *J. Org. Chem.* **2004**, *69*, 1151.

[7] Lei, Y. X.; Rappoport, Z. *J. Org. Chem.* **2002**, *67*, 6971.

[8] For example, see: (a) Hare, M. C.; Marimanikkupam, S. S.; Kass, S. R. *Int. J. Mass Spectrom. Ion Phys.* **2001**, *210/211*, 153. (b) Schroeder, D.; Loos, J.; Thissen, R.; Dutuit, O.; Mourgues, P.; Audier, H.-E.; Lifshitz, C.; Schwarz, H. *Angew. Chem., Int. Ed.* **2002**, *45*, 2748. (c) Decouzon, M.; Exner, O.; Gal, J.-F.; Maria, P.-C. *J. Org. Chem.* **1990**, *55*, 3980.

[9] Mishima, M.; Mustanir; Eventova, I.; Rappoport, Z. *J. Chem. Soc., Perkin Trans. 2* **2000**, 1505.

[10] Bartmess, J. E. In *NIST Chemistry WebBook, NIST Standard Reference Database* 69; Mallard, W. G., Linstrom, P. J., Eds.; National Institute of Standards and Technology: Gaithersburg, MD, 2003. http://webbook.nist.gov.

TABLE 1. Free Energy Changes of Proton Transfer Equilibria and Gas-Phase Acidities

acids	reference acids [$\Delta G°_{acid}$]^a	$\Delta G°$ ^{b}	selected $\Delta G°_{acid}$
YY′ in CH_2YY'			
$(CO_2CH_3)_2$	$C_6H_5CH_2CN$ [344.1]	−3.0	
	p-MeC_6H_4OH [343.4]	−2.1	
	CH_3COOH [341.1]	0.2	341.3
$(CO_2Me)CO_2CH_2CF_3$	$(CH_3CO)_2CH_2$ [336.7]	−3.0	
	p-$CF_3C_6H_4CH_2CN$ [332.9]	0.6	333.5
$(CO_2CH_2CF_3)_2$	$NCCH_2CO_2CH_2CF_3$ [324.7]	−0.5	
	$(CF_3)_3COH$ [324.0]	0.4	
	$CH_2(CN)_2$ [328.3]	−4.2	324.2
$(CN)CO_2CH_3$	$(CH_3CO)_2CH_2$ [336.7]	−3.4	
	m-$CF_3C_6H_4CH_2CN$ [335.3]	−0.8	
	p-$CF_3C_6H_4CH_2CN$ [332.9]	1.8	334.5
$(CN)CO_2CH_2CF_3$	$(CF_3)_3COH$ [324.0]	0.7	
	$(CF_3CH_2CO_2)_2CH_2$ [324.2]	0.5	
	$CF_3COCH_2COCH_3$ [322.0]	3.0	324.7
$(CN)CO_2CH(CF_3)_2$	$CF_3COCH_2COCH_3$ [322.0]	−4.3	
	C_6F_5OH [320.8]	−2.9	
	CF_3COOH [316.3]	0.7	317.5
YY′ in $PhNHCOCHYY'$			
$(CO_2CH_3)_2$	$CH_2(CN)_2$ [328.3]	−4.2	
	$(CF_3)_3COH$ [324.0]	0.1	324.1
$(CO_2Me)CO_2CH_2CF_3$	$NCCH_2CO_2CH(CF_3)_2$ [317.5]	0.3	
	CF_3COOH [316.3]	2.0	318.0
$(CO_2CH_2CF_3)_2$	CF_3COSH [312.5]	−1.0	
	$(CF_3CO)_2CH_2$ [310.3]	1.0	311.4
$(CN)CO_2CH_3$	$(CF_3CO)_2CH_2$ [310.3]	−1.3	
	$(CF_3CO)_2NH$ [307.5]	1.6	309.0
$(CN)CO_2CH_2CF_3$	$(CF_3CO)_2NH$ [307.5]	−3.5	
	$(C_3F_7CO)_2CH_2$ [305.3]	−1.3	304.0
$(CN)CO_2CH(CF_3)_2$	$(C_3F_7CO)_2CH_2$ [305.3]	−4.7	
	$(4\text{-}C_5F_4N)_2CHCN$ [302.2]	−1.0	
	$(CF_3SO_2)_2CH_2$ [301.5]	−0.5	301.0
$(CN)_2$	$(C_3F_7CO)_2CH_2$ [305.3]	−2.0	
	$(CF_3SO_2)_2CH_2$ [301.5]	1.2	303.0
YY′ in p-$BrC_6H_4NHCOCHYY'$			
$(CO_2CH_3)CO_2CH_2CF_3$	$NCCH_2CO_2CH(CF_3)_2$ [317.5]	−0.5	317.0
$(CO_2CH_2CF_3)_2$	$(CF_3CO)_2CH_2$ [310.3]	−0.9	
	$(CF_3CO)_2NH$ [307.5]	1.9	309.4
YY′ in i-$PrNHCOCHYY'$			
$(CO_2CH_3)_2$	p-$CF_3C_6H_4CH_2CN$ [332.9]	−1.6	
	p-$CF_3C_6H_4OH$ [330.1]	1.0	331.2
$(CO_2CH_3)CO_2CH_2CF_3$	$(CF_3)_3COH$ [324.0]	0.3	
	$CF_3COCH_2COCH_3$ [322.0]	2.3	324.3
$(CO_2CH_2CF_3)_2$	C_6F_5OH [320.8]	−3.3	
	CF_3COOH [316.3]	1.0	317.4
$(CN)CO_2CH_3$	CF_3COOH [316.3]	0.4	
	C_6F_5COOH [316.6]	0.4	317.0
$(CN)CO_2CH_2CF_3$	$(CF_3CO)_2CH_2$ [310.3]	−0.3	
	$(CF_3CO)_2NH$ [307.5]	2.3	310.0
$(CN)_2$	$(CF_3CO)_2CH_2$ [310.3]	−1.2	
	$(CF_3CO)_2NH$ [307.5]	1.8	309.2
cyclic CH_2YY'			
Meldrum acid (MA)	$CH_2(CO_2CH_2CF_3)_2$ [324.2]	0.7	
	$CH_3COCH_2COCF_3$ [322.0]	2.5	324.9
cyclopentanedione (CPD)	$CH_2(CN)_2$ [328.3]	−1.9	
	$NCCH_2CO_2CH_2CF_3$ [324.7]	1.9	326.5
indanedione (IND)	$CH_2(CN)_2$ [328.3]	−0.4	
	$NCCH_2CO_2CH_2CF_3$ [324.7]	3.0	327.9
cyclic-CONHR amides			
Meldrum acid N-Ph (MA-N-Ph)	$CF_3COCH_2COCH_3$ [322.0]	−3.4	
	$NCCH_2CO_2CH(CF_3)_2$ [317.5]	0.9	318.5
Meldrum acid N-C_6H_4Br-p	C_6F_5OH [320.8]	−3.0	317.8
Meldrum acid N-Pr-i (MA-N-Pr-i)	$CH_2(CN)_2$ [328.3]	−3.0	
	$NCCH_2CO_2CH_2CF_3$ [324.7]	0.7	325.4
dimedone N-Ph(DIM-N-Ph)	$CH_2(CN)_2$ [328.3]	−2.2	
	$(CF_3)COH$ [324.0]	2.0	326.1
cyclopentanedione N-Ph(CPD-N-Ph)	$CF_3COCH_2COCH_3$ [322.0]	−2.2	
	C_6F_5OH [320.8]	−0.9	319.9
indanedione-N-Ph(IND-N-Ph)	CF_3COOH [316.3]	−3.0	313.3

[a] NIST database, refs 10 and 11. [b] $\Delta G°$ for the proton transfer to the reference acid mentioned.

TABLE 2. Observed Acidities ($\Delta G°_{acid}$) and Calculated Thermodynamic Parameters (ΔH, ΔG, ΔS) at B3LYP/6-31+G*//B3LYP/6-31+G*, B3LYP/6-311+G*//B3LYP/6-311+G* (in Parentheses), and B3LYP/6-311+G//B3LYP/6-311+G** (in Brackets) for the Ionization at the C−H or O−H Sites**[a]

		calculated thermodynamic parameters for the ionization					
	observed	enol form[c]			amide or carbonyl form		
acids	$\Delta G°_{acid}$	$\Delta H°$	$\Delta G°$	$\Delta S°$	$\Delta H°$	$\Delta G°$	$\Delta S°$
YY′ in CH_2YY'							
$(CO_2Me)_2$	341.3	333.7	325.1	29.0	343.5	336.8	22.6
		(332.0)	(323.4)	(29.0)	(343.4)	(336.6)	(23.0)
		[336.6]	[327.8]	[29.3]	[344.0]	[337.1]	[23.1]
$(CO_2Me)CO_2CH_2CF_3$	333.5	324.4	316.2	27.7	333.7	328.0	18.9
$(CO_2CH_2CF_3)_2$	324.2	315.0	306.0	30.0	324.5	317.4	24.1
$(COMe)_2$	336.7[d]	339.7	331.8	26.8	337.1	330.2	23.4
		(338.4)	(330.5)	(26.5)	(337.3)	(330.1)	(23.9)
		[342.8]	[334.3]	[28.6]	[337.8]	[330.3]	[25.0]
$(CN)CO_2Me$	334.5	316.8	309.4	24.9	335.7	329.3	21.2
		(315.9)	(308.5)	(24.9)	(335.5)	(328.9)	(21.9)
		[319.9]	[312.4]	[25.0]	[336.0]	[329.4]	[22.2]
$(CN)CO_2CH_2CF_3$	324.7	306.1	299.0	23.8	324.9	318.1	22.8
$(CN)CO_2CH(CF_3)_2$	317.5	294.9	287.0	26.6	316.7	309.9	22.8
$(CN)_2$	328.3[d]				329.4	322.0	24.9
					(329.2)	(321.8)	(24.9)
					[329.6]	[321.8]	[26.3]
YY′ in PhNHCOCHYY′ [b]							
$(CO_2Me)_2$	324.1	328.7	320.5	27.6	327.1	320.6	21.8
$(CO_2Me)CO_2CH_2CF_3$	317.9	322.9[f]	314.8[f]	27.2[f]	319.7	313.6	20.6
		322.4[g]	314.4[g]	26.7[g]			
$(CO_2CH_2CF_3)_2$	311.4	316.2	307.2	30.0	312.2	306.1	20.3
$(CN)CO_2Me$	309.0	312.5[g]	305.0[g]	25.2[g]	309.4	303.4	20.3
		308.5[f]	301.4[f]	23.8[f]			
$(CN)CO_2CH_2CF_3$	304.0	306.3[g]	298.9[g]	24.5[g]	301.7	295.2	21.7
		302.5[f]	295.3[f]	24.5[f]			
$(CN)CO_2CH(CF_3)_2$	301.5	301.8[g]	294.1[g]	25.6[g]	295.9	290.3	18.8
		298.3[f]	291.0[f]	24.7[f]			
$(CN)_2$	303.0	299.9	292.9	23.3	303.4	296.6	22.9
YY′ in *p*-$BrC_6H_4NHCOCHYY'$ [b]							
$(CO_2Me)CO_2CH_2CF_3$	317.0	319.4[f]	310.6[f]	29.5[f]	316.2	310.1	20.6
$(CO_2CH_2CF_3)_2$	309.4	312.4	303.3	30.6	308.8	302.4	21.6
YY′ in *i*-PrNHCOCHYY′ [b]							
$(CO_2Me)_2$	331.2	336.7	328.0	29.2	334.0	328.0	20.2
		(334.6)	(326.3)	(28.0)	(334.3)	(328.2)	(20.4)
		[339.5]	[330.9]	[28.9]	[334.9]	[328.1]	[20.8]
$(CO_2Me)CO_2CH_2CF_3$	324.3	330.5[f]	321.7[f]	29.5[f]	325.9	319.5	21.4
		330.0[g]	321.0[g]	30.2[g]			
$(CO_2CH_2CF_3)_2$	317.5	323.4	314.7	29.4	318.2	312.1	20.5
$(CN)CO_2Me$	317.0	321.0[g]	312.7[g]	27.6[g]	316.5	310.1	21.6
		(319.6)[g]	(311.4)[g]	(27.5)[g]	(316.8)	(310.7)	(20.6)
		[324.0][g]	[315.7][g]	[27.6][g]	[317.5]	[311.7]	[19.4]
		316.4[f]	308.4[f]	27.0[f]			
$(CN)CO_2CH_2CF_3$	309.9	314.3[g]	306.2[g]	27.3[g]	308.3	302.1	21.1
		310.4[f]	302.3[f]	26.4[f]			
$(CN)CO_2CH(CF_3)_2$		309.2[g]	301.1[g]	27.2[g]	302.2	296.7	18.2
		305.5[f]	297.6[f]	26.5[f]			
$(CN)_2$	309.2	307.6	299.8	25.9	310.3	303.3	23.5
		(306.7)	(299.0)	(26.1)	(310.3)	(303.3)	(23.5)
		[310.7]	[302.8]	[26.3]	[311.0]	[303.9]	[23.8]
cyclic CH_2YY'							
Meldrum acid (MA)	324.9	314.7[e]	307.3[e]	24.8[e]	328.0	320.9	23.6
		(313.9)[e]	(306.5)[e]	(24.8)[e]	(327.8)	(320.7)	(23.6)
		[318.0][e]	[310.6][e]	[24.8][e]	[328.4]	[321.4]	[23.6]
dimedone (DIM)	331.2[d]	326.2[e]	318.8[e]	25.0[e]	331.8	324.8	23.6
		(325.6)[e]	(318.2)[e]	(25.0)[e]	(331.9)	(324.8)	(23.7)
		[329.6][e]	[322.2][e]	[24.9][e]	[332.5]	[325.5]	[23.7]
cyclopentanedione (CPD)	326.5	324.1[e]	316.6[e]	25.2[e]	328.6	321.8	22.7
indanedione (IND)	327.9	317.8[e]	310.3[e]	25.3[e]	332.5	324.9	25.6
cyclic-CONHR amides							
Meldrum acid *N*-Ph (MA-*N*-Ph)	318.9	321.6	313.3	27.6	310.0	303.0	23.6
		(319.6)	(311.5)	(27.1)	(310.2)	(302.2)	(23.5)
		[324.1]	[316.0]	[27.3]	[310.7]	[303.7]	[23.5]
		319.9[e]	311.5[e]	28.0[e]			
		(317.8)[e]	(309.5)[e]	(27.8)[e]			
		[322.7][e]	[314.5][e]	[27.8][e]			
Meldrum acid *N*-C_6H_4Br-*p*	317.8	317.3	308.9	28.2	306.3	299.3	23.4
		316.0[e]	307.6[e]	28.2[e]			

Table 2. (Continued)

		calculated thermodynamic parameters for the ionization					
	observed	enol form[c]			amide or carbonyl form		
acids	$\Delta G°_{acid}$	$\Delta H°$	$\Delta G°$	$\Delta S°$	$\Delta H°$	$\Delta G°$	$\Delta S°$
cyclic-CONHR amides (continued)							
Meldrum acid *N*-Pr-*i*	325.4	331.2	323.1	27.0	316.2	310.3	19.8
(MA-*N*-Pr-*i*)		(329.2)	(321.2)	(26.8)	(316.3)	(310.5)	(19.6)
		[333.7]	[325.6]	[27.0]	[317.1]	[310.8]	[21.0]
		328.7^{e}	320.8^{e}	26.4^{e}			
dimedone *N*-Ph	319.9	330.0	321.3	29.2	316.0	309.4	22.1
(DIM-*N*-Ph)		331.0^{e}	322.1^{e}	29.8^{e}			
cyclopentanedione *N*-Ph	326.1	321.5	313.9	25.5	306.6	299.9	22.2
(CPD-*N*-Ph)		323.6^{e}	315.4^{e}	27.5^{e}			
indanedione-*N*-Ph	313.3	318.7	310.8	26.5	310.4	303.8	22.1
(IND-*N*-Ph)		318.3^{e}	310.3^{e}	26.9^{e}			

[a] $\Delta H°$ and $\Delta G°$ are in kcal mol^{-1}, and $\Delta S°$ is in cal mol^{-1} K^{-1}. Thermodynamic quantities of the proton are 1.481 kcal mol^{-1}, −6.275 kcal mol^{-1}, and 26.014 cal mol^{-1} K^{-1} for *H*, *G*, and *S*, respectively. [b] Amide structure is drawn for convenience. [c] Data for the enol form of the amide unless otherwise noted. [d] NIST database. Ref 10. [e] Data for the enol form on the carbonyl group. [f] Data for the (*E*)-enol form. [g] Data for the (*Z*)-enol form.

malonate $CH_2(CO_2Me)_2$ ($\Delta G°_{acid} = 341.3$ kcal/mol) and the stronger acid is $CH_2(CN)CO_2CH(CF_3)_2$) ($\Delta G°_{acid} = 317.5$ kcal/mol), i.e., the $\Delta G°_{acid}$ spans ca. 24 kcal/mol. (b) Analogously in the *N*-Ph derivatives (series B), the $(CO_2Me)_2$ derivative is the weaker acid and the $CN(CO_2CH(CF_3)_2)$ derivative the stronger acid ($\Delta G°_{acid}$ 324.1 and 302.7 kcal/mol, respectively). The effect of a *p*-Br substituent in the ring is minor: the acidity increases by 0.9 and by 2.0 kcal/mol for the $CO_2Me(CO_2CH_2CF_3)$ and the $(CO_2CH_2CF_3)_2$, respectively.

(c) In the *N*-*i*-Pr series (C), the $(CO_2Me)_2$ derivative is again the weaker acid, and the $(CN)_2$ derivative the stronger acid; the $\Delta G°_{acid}$ values span 22 kcal/mol. The $CN(CO_2CH(CF_3)_2)$ derivative is not available.

The series B compounds are 6−8 kcal/mol stronger acids than their series C analogues. A plot of the $\Delta G°_{acid}$ values for the *N*-*i*-Pr series vs the *N*-Ph series is linear (slope = 1.02; $R^2 = 0.998$) (Figure 1). A point for Meldrum's acid (MA) is also on the line. The black points on the plot are for the two weaker acidic diesters and are on the correlation line, although the compounds have the amide structure in the solid-state, whereas the other compounds are enols in the solid state.

(d) As summarized in Figure 2, there is a near additivity effect of replacing a CO_2Me by a $CO_2CH_2CF_3$ group by 6.5 ± 0.3 kcal/mol in series B and C and of 8.5 ± 0.8 kcal/mol in series A. Replacement of a CO_2Me by a CN increases the acidity by 6.9 ± 0.9 kcal/mol, except that in series B and C, the first $CO_2Me \rightarrow CN$ replacement increase the acidity much more, by 14.2 and 15.1 kcal/mol, respectively.

(e) Plots of the observed $\Delta G°_{acid}$ (enols/amides) values vs the corresponding $\Delta G°_{acid}(CH_2YY')$ values are not linear for all Y,Y′ combinations. Each subfamily of compounds seems to give its own correlation. For the *N*-Ph derivatives, three lines are clearly obtained for the limited number of compounds available. The three open-chain diesters are on one line with a slope of 0.74 ($R^2 = 0.999$). The three cyanoesters are on another line below it with a smaller slope of 0.47 ($R^2 = 0.997$). The single point for the $(CN)_2$ systems is below these lines (Figure 3a).

For the *N*-Pr-*i* system, a similar behavior is observed, with corresponding slopes of 0.80 ($R^2 = 0.997$) for the diester and 0.71 for the two points available for $CN(CO_2R)$, and the points for $(CN)_2$ and MA are below and above these lines, respectively (Figure 3b).

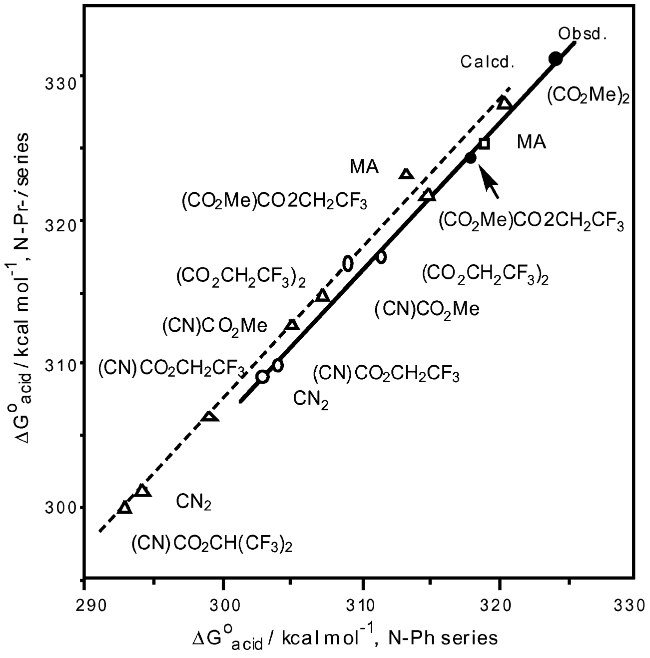

FIGURE 1. Plot of the observed (○, □, solid line, slope 1.02, $R^2 = 0.993$) and the calculated (Δ, dashed line, slope 1.04, $R^2 = 0.993$), $\Delta G°_{acid}$ values for the *N*-Pr-*i* series vs those for the *N*-Ph series. The black points are for systems having the amide structure in the solid, and the open circles are for systems with an enol structure in the solid.

Figure 3a also includes data for four compounds of groups D and E. X-ray data show that the derivatives of the 1,3-diketones dimedone (DIM) and 1,3-cyclopentanedione (CPD) exist in the solid as enols on a ring carbonyl group, which are substituted at C2 by a CONHPh group. Hence, they are not enols of amides species. They appear as the top line in Figure 3a above the enols of amides, together with the point for Meldrum's acid (slope 1.23; $R^2 = 0.995$). The point for the IND derivative appears on the diester line. IND is the 4,5-benzo derivative of CPD, and its corresponding point is expected to be on the "β,β-dioxo" derivatives line, while the cyclic

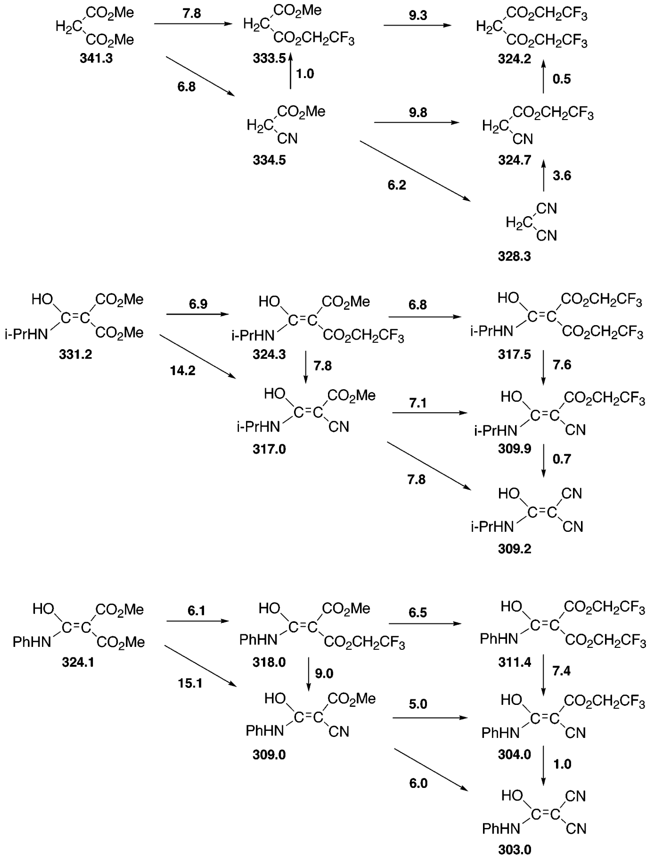

FIGURE 2. Changes in the $\Delta G°_{acid}$ values for replacing a CO_2-Me group by a $CO_2CH_2CF_3$ or a CN group.

diester Meldrum's acid (MA) formally belongs to the diesters line so that their positions seem to be inverted, at least formally. However, the IND derivative is an enol of amide in the solid state.[12] A *p*-Br substituent increases the $\Delta G°_{acid}$ of Meldrum's acid enol by only 1.0 kcal/mol, similar to its effect in series B.

Calculated Acidities. The acidities of all the systems were calculated at the B3LYP/6-31+G* level with the neutral acid calculated both as the enol and as the amide. Frequency calculations gave the entropy. Also calculated was acetylacetone for which experimental data are available[10] but whose corresponding derived amide was not studied. The data are given in Table 2.

Due to a few kcal/mol systematic discrepancies between the calculated and the observed values (see below), several systems were calculated also at the higher B3LYP/6-311+G*//B3LYP/6-311+G* and the B3LYP/6-311+G**//B3LYP/6-311+G** levels in order to observe if the discrepancies would be reduced. The data are given in parentheses and brackets, respectively, in Table 2 and other tables. The differences in $\Delta G°_{acid}$ increase at the B3LYP/6-311+G*//B3LYP/6-311+G* level, but at the B3LYP/6-311+G**//B3LYP/6-311+G** level, the discrepancies for the enols are significantly reduced. In contrast, the differences for compounds CH_2YY' are only slightly affected, except for the enol of acetylacetone (see below). The improvements are mainly due to the $\Delta H°_{acid}$ terms since the $\Delta S°_{acid}$ terms are much less affected.

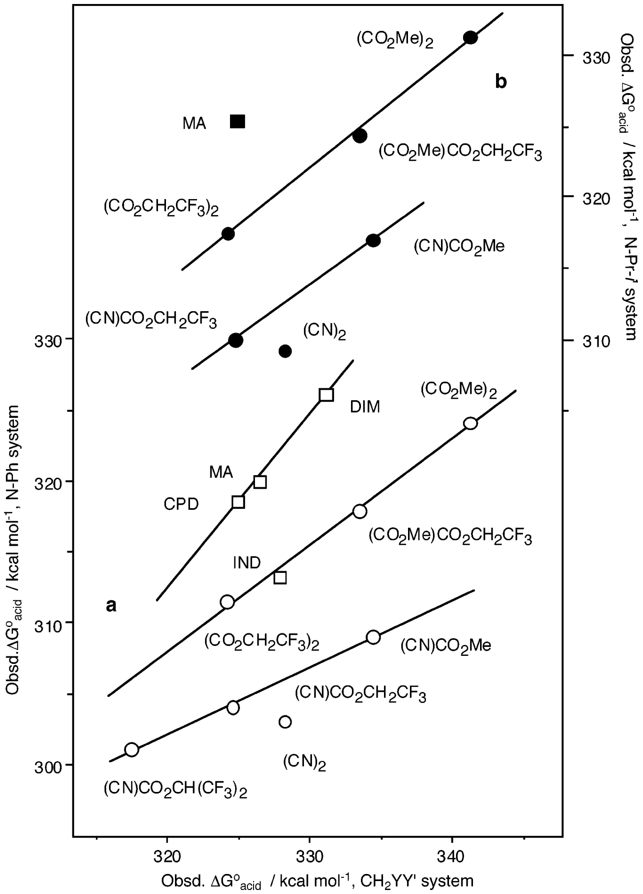

FIGURE 3. (a) Plot of the observed $\Delta G°_{acid}$ values for the *N*-Ph systems vs $\Delta G°_{acid}$ values for CH_2YY' (open circles and squares, lower scale and lower three lines). Top line: cyclic systems excluding IND (slope 1.23; $R^2 = 0.995$). Middle line: diesters + IND (slope 0.74; $R^2 = 0.995$). Bottom line: cyanoesters (slope 0.47; $R^2 = 0.997$). (b) Plot of the observed $\Delta G°_{acid}$ values for the *N*-Pr-*i* systems vs $\Delta G°_{acid}$ values for CH_2YY' (black circles and squares, upper scale and upper two lines). Top line: diesters (slope 0.80; $R^2 = 0.997$). Bottom line: cyanoesters (slope 0.71).

The calculated vs the observed $\Delta G°_{acid}$ values were plotted for the various subseries. A plot of the *N*-*i*-Pr system, with the amide as the ionizing species is linear for all six noncyclic systems investigated (slope = 1.13; $R^2 = 0.994$). The point for MA is well below the line. When the calculated $\Delta G°_{acid}$ values for the enols are used, a linear plot is obtained with a slope of 1.04 ($R^2 = 0.995$), with the points for MA and $(CN)_2$ below the correlation line. If the calculated value for the $(CN)_2$-amide replaces that for the $(CN)_2$-enol, the deviation is reduced from 5.7 to 2.2 kcal/mol (Figure 4).

A similar plot for the open-chain *N*-Ph system for the precursor amides is linear, with deviation of the $(CN)_2$ point (slope 1.27; $R^2 = 0.981$). Of the cyclic compounds, the point for IND is near the line, but those for CPD, MA, and DIM are below it. Using calculated data for the precursor enols, we found the points for the stronger acid systems of $(CN)_2$, MA, CPD, and DIM to be somewhat below the line of the other points, which has a slope of

---

(11) Koppel, I. A.; Taft, R. W.; Anvia, F.; Zhu, S.-Z.; Hu, L.-Q.; Sung, K.-S.; DesMartenau, D. D.; Yagupolskii, L. M.; Yagupolskii, Y. L.; Valsov, V. M.; Notario, R.; Maria, P.-C. *J. Am. Chem. Soc.* **1994**, *116*, 3047.

(12) Mukhopadhyaya, J. K.; Rappoport, Z. Unpublished results.

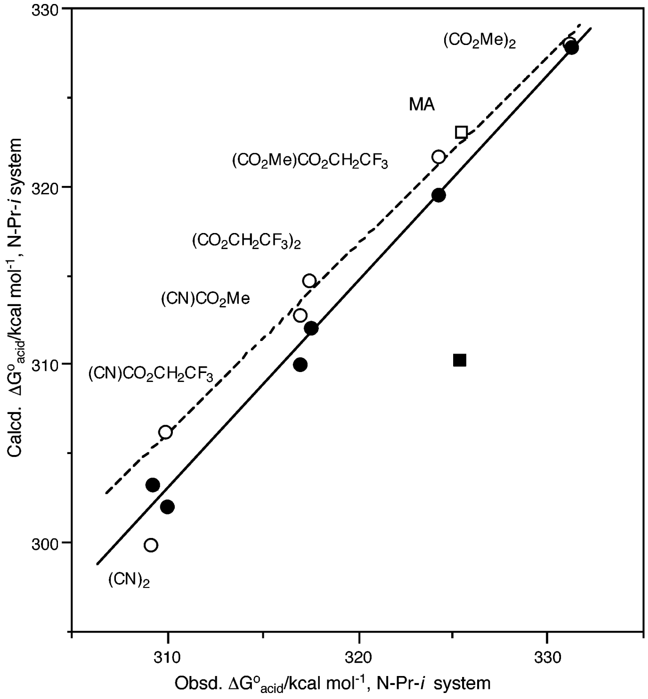

FIGURE 4. Plot of the calculated values vs the observed $\Delta G°_{acid}$ values for the amides (black points and solid line; slope 1.13; $R^2 = 0.994$) and the enols (open points and broken line; slope ((excluding $(CN)_2$) 1.04; $R^2 = 0.995$) for the *N*-Pr-*i* systems.

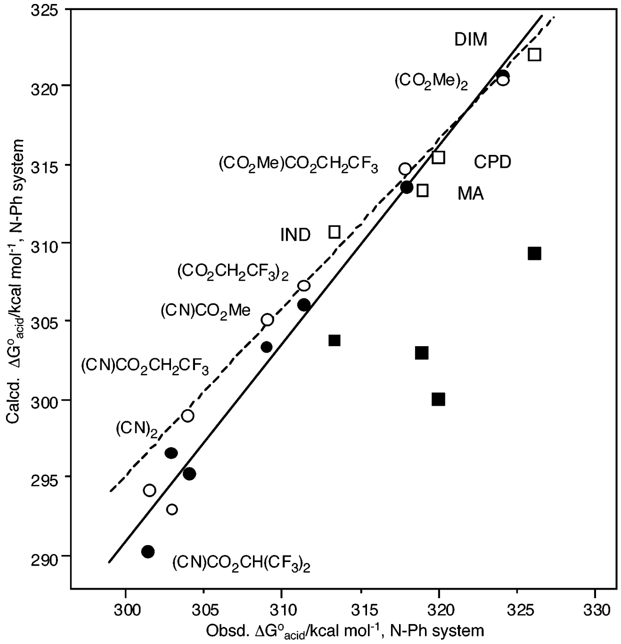

FIGURE 5. Plot of the calculated values vs the observed $\Delta G°_{acid}$ values for the amides (black points and line; slope 1.27; $R^2 = 0.981$) and the enols (open points and broken line; slope 1.07; $R^2 = 0.998$, points for $(CN)_2$ and $CN(CO_2CH(CF_3)_2)$ excluded) for the *N*-Ph systems.

1.07 ($R^2 = 0.998$, excluding the $(CN)_2$ and $CN(CO_2CH(CF_3)_2)$ points) (Figure 5).

The data of Figures 4 and 5 together with those for the cyclic compounds are combined in Figure S1 in Supporting Information, where the solid line with a slope of unity is that expected for a perfect coincidence between the calculation and the experiment. Most points for all families of the enols are on or near a dashed line that is nearly parallel and ca. 4 kcal/mol below the solid line. In contrast, most of the points calculated for the amides are below this line except for the two $(CN)_2$-substituted derivatives, where the points for the amides are above those for the enols and closer to this line.

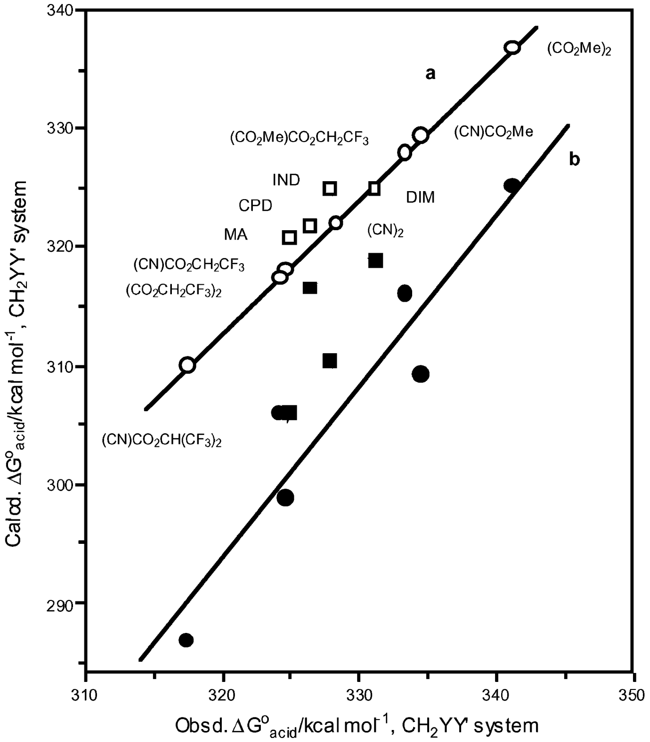

FIGURE 6. Plot of the calculated values vs the observed $\Delta G°_{acid}$ values for the CH_2YY' systems. (a) Calculated for the nonenolic form (open circles and squares; for circles only, slope 1.13; $R^2 = 1.000$; for all points, slope 1.09; $R^2 = 0.962$). (b) Calculated for the enolic form on the ester or dioxo group (black circles and squares; for circles, slope 1.45; $R^2 = 0.900$; for all points, slope 1.23; $R^2 = 0.404$).

The plot of the calculated values for the nonenolic form vs the observed $\Delta G°_{acid}$ values for CH_2YY' systems (Figure 6a) displays a perfect linearity (slope 1.13; $R^2 = 1.000$) for the open-chain species. The point for DIM is almost on the line, whereas those for MA, CPD, and IND are 2−4 kcal/mol above it. A similar plot calculated for the enolic form on the ester or on a keto carbonyl group shows a poorer correlation (Figure 6b).

A calculated $\Delta G°_{acid} - \Delta G°_{acid}$ plot for the enol form for the *N*-Pr-*i* vs the *N*-Ph series is linear for all the open-chain systems (slope 1.04; $R^2 = 0.993$), and the point for MA is 3 kcal/mol above the line. As shown in Figure 1, the plot resembles the corresponding plot for the observed $\Delta G°_{acid}$ values.

Likewise, the calculated $\Delta G°_{acid}$(*N*-*i*-Pr) for enols vs the calculated $\Delta G°_{acid}(CH_2YY')$ plot (Figure 7a) resembles the corresponding observed vs observed $\Delta G°_{acid}$ plot (Figure 3b) in displaying a top line for the three open-chain diesters and Meldrum's acid (slope 0.69; $R^2 = 0.999$), a lower line for the three cyanoesters (slope 0.60; $R^2 = 1.000$), and a still lower point for the $(CN)_2$ system. The MA point is on the line of Figure 7a. A corresponding

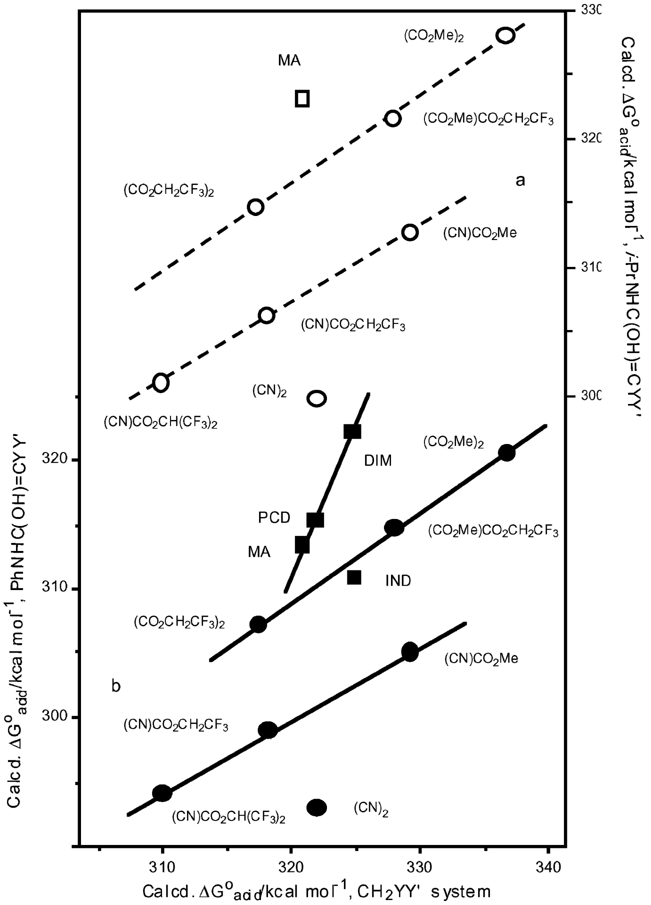

FIGURE 7. (a) Plot of the calculated $\Delta G°_{\mathrm{acid}}$ (N-Pr-i) values vs the calculated $\Delta G°_{\mathrm{acid}}$ (CH$_2$YY′) values (open circles and squares, right scale and top two lines). Top line: diesters (slope 0.69; $R^2 = 0.999$); Bottom line: cyanoesters (slope 0.60; $R^2 = 1.000$); (b) Plot of the calculated $\Delta G°_{\mathrm{acid}}$ (N-Ph) vs the calculated $\Delta G°_{\mathrm{acid}}$ (CH$_2$YY′) values (black circles, left scale and bottom three lines). Top line: MA,CPD, DIM (slope 2.28; $R^2 = 1.000$). Middle line: diesters (slope 0.68; $R^2 = 1.000$). Bottom line: cyanoesters (slope 0.56; $R^2 = 1.000$).

plot for the calculated $\Delta G°_{\mathrm{acid}}$($N$-Pr-$i$) for the amide vs the calculated $\Delta G°_{\mathrm{acid}}$(CH$_2$YY′) values is similar except that the point for MA is below the diester line and that for (CN)$_2$ below the cyanoester line.

The calculated $\Delta G°_{\mathrm{acid}}$($N$-Ph) vs the calculated $\Delta G°_{\mathrm{acid}}$(CH$_2$YY′) plot for both carbonyl forms (Figure 7b) displays a spread of points similar to that for the corresponding observed $\Delta G°_{\mathrm{acid}}$ vs observed $\Delta G°_{\mathrm{acid}}$ line (Figure 3a). The esters are on one line, and the IND point is close to it (slope 0.68; $R^2 = 1.000$). The cyanoesters are on a lower line (slope 0.56; $R^2 = 1.000$), and the (CN)$_2$ point is below both lines. MA, CPD, and DIM are on a much steeper line (slope 2.28; $R^2 = 1.000$). A similar plot for the N-Ph systems calculated for the amide form is linear for the cyanoesters, but the diester line is curved.

A plot of the calculated $\Delta G°_{\mathrm{acid}}$ values for the amides against the calculated $\Delta G°_{\mathrm{acid}}$ values for the enols (Figure 8) for all systems shows a large scatter, but correlations for subgroups are observed. Six of the seven i-Pr systems give excellent linearity (Figure 8a: slope 1.12; $R^2 = 0.999$), and the (CN)$_2$ point deviates. Eight of the nine points observed for the N-Ph/N-p-BrC$_6$H$_4$ systems gave very good linearity (Figure 8b: slope = 1.15; $R^2 = 0.995$, strong deviation of the (CN)$_2$ point). No linear correlation was observed for the cyclic CH$_2$YY′ systems (Figures 8c: slope = 0.14; $R^2 = 0.146$) and the N-Ph-cyclic enols (Figure 8d: slope 0.61; $R^2 = 0.600$). The enols of the open-chain CH$_2$YY′ systems gave relatively poor correlation (Figure 8e: slope 0.70; $R^2 = 0.895$).

Finally, in a plot of $\Delta G°_{\mathrm{acid}}$(CH$_2$YY′) values in DMSO vs the gas-phase values (Figure 9), the available data for CH$_2$(CN)$_2$, CH$_2$(CO$_2$Me)$_2$, MA, and DIM are approximately on a line including also CH$_2$(COMe)$_2$, CH$_2$(CO$_2$-

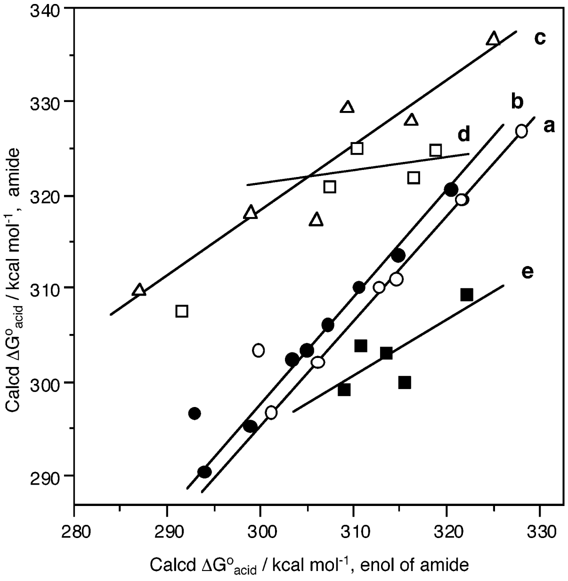

FIGURE 8. Plot of the calculated $\Delta G°_{\mathrm{acid}}$ values of the amide vs those of the enol of amide. Open circles: N-Pr-i (a) (slope 1.12; $R^2 = 0.999$, excluding (CN)$_2$). Closed circles: N-Ph and N-C$_6$H$_4$Br-p (b) (slope 1.15, $R^2 = 0.995$, excluding (CN)$_2$). Triangles: CH$_2$YY′ (c) (slope 0.70, $R^2 = 0.895$). Open squares: cyclic systems (d) (slope 0.14, $R^2 = 0.146$). Closed squares: Ph-substituted cyclic systems (e) (slope 0.61, $R^2 = 0.600$).

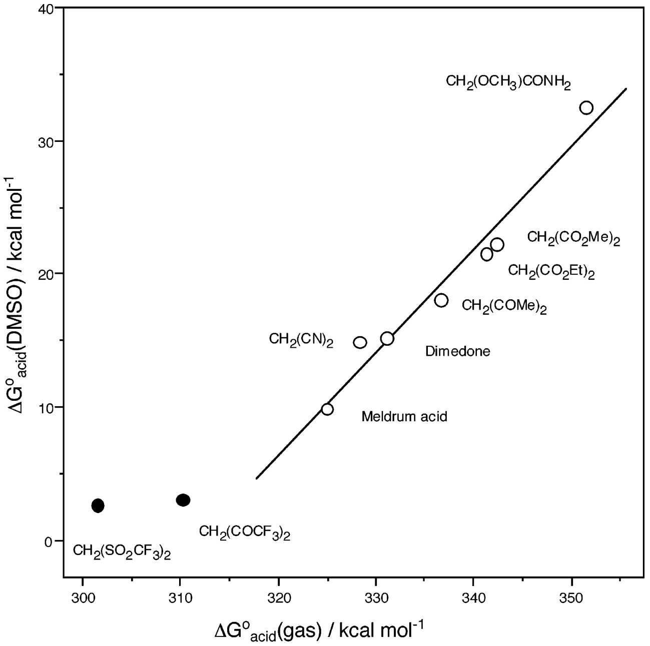

FIGURE 9. Plot of the observed $\Delta G°_{\mathrm{acid}}$(CH$_2$YY′) values in DMSO vs the gas-phase values (slope 0.64; $R^2 = 0.957$).

Et)$_2$, and MeOCH$_2$(CONH$_2$) (slope 0.64; $R^2 = 0.957$). The plot breaks and gives a plateau for highly acidic fluoro systems taken from the literature.[10,11,13]

K_{enol} Values and Related Thermodynamic Parameters. K_{enol} values and the thermodynamic parameters, $\Delta G°_{AE}$, $\Delta H°_{AE}$, and $\Delta S°_{AE}$, for the amide ⇌ enol equilibria are calculated in Table 3 from eq 2 and the data in Table 2. The positive $\Delta G°_{AE}$ (CH$_2$YY′) values and the pK_{enol} values of 5.2−16.9 indicate a lower stability of the enol than of the CH$_2$YY′. The main contributors to the $\Delta G°_{AE}$ values are the $\Delta H°_{AE}$ values. Except for the (CN)$_2$ derivatives, the pK_{enol} values for *N*-Ph and *N*-Pr-*i* amido derivatives are negative, i.e., the enol is more stable than the amide in the gas phase.

In a $\Delta G°_{AE}$ vs $\Delta G°_{acid}$ plot, the points for the CH$_2$YY′ systems are spread: those for the cyanoester are in one region, and those for the diesters are in another (Figure S2 in Supporting Information). Two regions, one for the cyclic CH$_2$YY′ and one for their *N*-Ph and *N*-Pr-*i* derivatives, were also observed (Figure S3 in Supporting Information). In contrast, the plots for the *N*-Ph and *N*-Pr-*i* systems are approximately linear (*N*-Ph: slope 0.17; $R^2 = 0.792$; *N*-Pr-*i*: slope 0.18; $R^2 = 0.935$) except that the (CN)$_2$ points are above the correlation lines (Figure 10).

Structures and Charge Distributions in the CH$_2$YY′, Amides, Enols, and Anions. The calculated geometries of several representative enols, amides, and anions are shown in Figures 11a−c. The rest are in Figure S4 in Supporting Information. The optimized bond lengths for all the noncyclic species of series B and C are given in Table 4. The corresponding parameters for the three cyclic compounds (series D and E), including the enols on both the amide and the β-carbonyl group, are given in Table S1 in Supporting Information. The corresponding parameters for the carbon acids CH$_2$YY′, the anions −CHYY′, and the enols on the carbonyl group for the noncyclic and cyclic species are given in Tables S2 and S3 in Supporting Information.

The ranges of the bond angles are shown schematically in Figure 11d for the *N*-Ph derivatives. The nitrogen is planar in both the enols and the anions, as well as for the *N*-Pr-*i* enols, but the sum of the angles around it is ca. 5° smaller than 360° in the anions. C$_\alpha$ and C$_\beta$ are planar in both the enols and the anions of both species.

The following generalizations emerge from the tables of bond lengths: (i) For the trisubstituted systems, the O−H is cis to the more basic ester group in the diesters or to the single ester group in the cyanoesters.

(ii) The O···O distances of 2.459−2.481 Å in the diesters and 2.532−2.567 Å in the cyanoesters and the N···O distances of 2.610−2.634 Å are indicative of very strong hydrogen bonds, in line with the experimental values.[6] Most of the O−H bond lengths are in the expected range. The nonbonded O−H···O distances indicate an unsymmetrical O−H···O bond. The long O−H···N(C) distances of >2.7Å in the dicyano derivatives (Table S3) indicate the absence of intramolecular hydrogen bonding.

(iii) The CO group in the amide PhNHCO(CN)$_2$ is kept as far as possible from the cyano groups, which are in anti and gauche relationships to it.

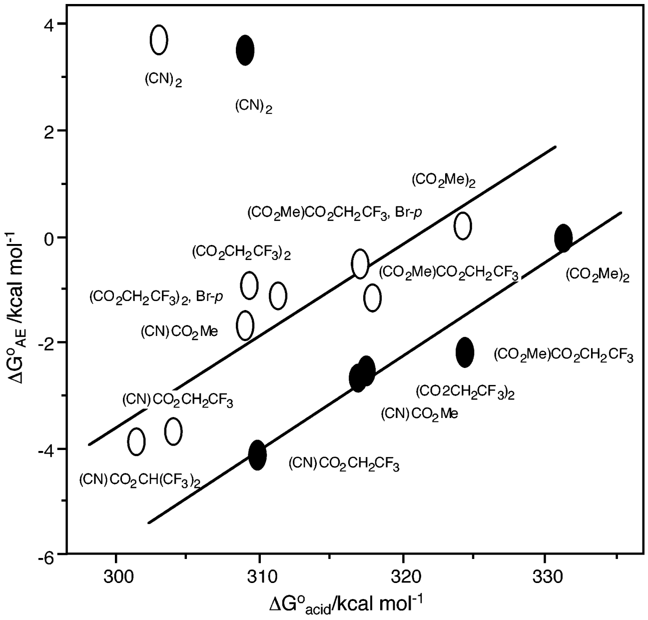

FIGURE 10. Plot of the calculated $\Delta G°_{AE}$ against the experimental $\Delta G°_{acid}$ values for the corresponding Y′YCHCONHR species. Open circles, *N*-Ph systems. Slope = 0.17; $R^2 = 0.792$. Filled circles: *N*-Pr-*i* systems. Slope = 0.18; $R^2 = 0.935$.

(iv) The double bond lengths in the enols are long (1.403−1.447 Å), whereas the single bonds to Y, Y′, O, and N are shorter than a regular single bond (e.g., the C−CN bond is 1.416 Å), indicating partial single bonds and partial double bonds, respectively (Table 4).

(v) The N−H bond lengths in all species are approximately the same, with somewhat longer values for the enols. The N−R bonds are longer by ca. 0.05Å for R = *i*-Pr than for R = Ph for the enols of amides and slightly longer for the enolate anion.

(vi) The N−C(=O) bonds of the amides are somewhat longer than the N−C(−O) bonds of the enols. These bonds are elongated in the anions compared with the neutral species.

(vii) The C−C$_{EWG}$ bonds in the CH$_2$YY′ are normal for the C$_{sp^3}$−C$_{sp^2}$(COOR) and the C$_{sp^3}$−C$_{sp}$(CN) bonds, respectively, but in the derived anions they are significantly shorter.

(viii) The CO−C$_\beta$ bonds in the amides are 1.552−1.583 Å, longer than C$_{sp^3}$−C$_{sp^3}$ bonds and the CO−C$_\beta$ bond of 1.522 Å in CH$_3$CO−NHR (R = Ph, *i*-Pr). The bond length increases with the increased electron-withdrawal by the β-substituents. The longest bonds of 1.582 and 1.583 Å are for the *N*-Pr-*i* and *N*-Ph (CN)$_2$-substituted systems.

(ix) The amide C=O bond is slightly elongated in the enolate ion than in the amide.

(x) In the trisubstituted systems, the bond lengths to the EWGs in the enolate ions do not differ much from those in the enols.

(xi) The compounds with Y, Y′ = (CN)$_2$ show shorter C$_\beta$−C$_{EWG}$, longer C−O(H), and shorter O−H bonds than in the other enols.

Charges. Calculated natural charges of the anions, enols, and amides for series B and C are given in Table 5. For series D and E and the cyclic and noncyclic CH$_2$YY′, they are in Tables S4 and S5 in Supporting Infor-

---

(13) Bordwell, F. G. *Acc. Chem. Res.* **1988**, *21*, 456.

TABLE 3. Calculated Thermodynamic Parameters at B3LYP/6-31+G*//B3LYP/6-31+G*, B3LYP/6-311+G*//B3LYP/6-311+G* (in Parentheses), and B3LYP/6-311+G//B3LYP/6-311+G** (in Brackets) for the Amide Enol Equilibria**[a]

acids	$\Delta H°_{AE}$	$\Delta G°_{AE}$	$\Delta S°_{AE}$
YY′ in CH_2YY'			
$(CO_2Me)_2$	9.8	11.7	−6.4
	(11.4)	(13.2)	(−6.0)
	[7.5]	[9.3]	[−6.2]
$(CO_2Me)CO_2CH_2CF_3$	9.3	11.8	−8.8
$(CO_2CH_2CF_3)_2$	9.5	11.4	−5.9
$(COMe)_2$	−2.6	−1.6	−3.4
	(−1.1)	(−0.4)	(−2.6)
	[−5.0]	[−3.9]	[−3.6]
$(CN)CO_2Me$	18.9	19.9	−3.7
	(19.6)	(20.4)	(−3.0)
	[16.1]	[17.0]	[−2.9]
$(CN)CO_2CH_2CF_3$	18.8	19.1	−1.0
$(CN)CO_2CH(CF_3)_2$	21.8	22.9	−3.8
YY′ in PhNHCOCHYY′			
$(CO_2Me)_2$	−1.6	0.1	−5.8
$(CO_2Me)CO_2CH_2CF_3$	−3.2^b	−1.2^b	−6.6^b
	−2.7^c	−0.8^c	−6.0^c
$(CO_2CH_2CF_3)_2$	−4.0	−1.1	−9.7
$(CN)CO_2Me$	−3.1^c	−1.7^c	−4.9^c
	0.9^b	1.9^b	−3.5^b
$(CN)CO_2CH_2CF_3$	−4.6^c	−3.7^c	−2.8^c
	−0.8^b	−0.1^b	−2.8^b
$(CN)CO_2CH(CF_3)_2$	−5.9^c	−3.8^c	−6.8^c
	−2.5^b	−0.7^b	−5.9^b
$(CN)_2$	3.5	3.7	−0.4
YY′ in *p*-$BrC_6H_4NHCOCHYY'$			
$(CO_2Me)CO_2CH_2CF_3$	−3.2^b	−0.5^b	−8.9^b
$(CO_2CH_2CF_3)_2$	−3.6	−0.9	−9.0
YY′ in *i*-PrNHCOCHYY′			
$(CO_2Me)_2$	−2.7	0.0	−9.0
	(−0.3)	(1.9)	(−7.6)
	[−4.6]	[−2.2]	[−8.1]
$(CO_2Me)CO_2CH_2CF_3$	−4.6^b	−2.2^b	−8.1^b
	−4.1^c	−1.5^c	−8.8^c
$(CO_2CH_2CF_3)_2$	−5.2	−2.5	−8.9
$(CN)CO_2Me$	−4.5^c	−2.6^c	−6.0^c
	(−2.8)^c	(−0.7)^c	(−6.9)^c
	[−6.5]^c	[−4.1]^c	[−8.2]^c
	0.1^b	1.7^b	−5.4^b
YY′ in *i*-PrNHCOCHYY′ (continued)			
$(CN)CO_2CH_2CF_3$	−6.0^c	−4.1^c	−6.3^c
	−1.8^b	−0.2^b	−5.4^b
$(CN)CO_2CH(CF_3)_2$	−7.1^c	−4.4^c	−9.0^c
	−3.3^b	−0.8^b	−8.3^b
$(CN)_2$	2.7	3.5	−2.4
	(3.6)	(4.3)	(−2.6)
	[0.4]	[1.1]	[−2.4]
YY′ in cyclic CH_2YY'			
Meldrum acid	13.3	13.6	−1.2
	(13.9)	(14.2)	(−1.2)
	[10.4]	[10.7]	[−1.2]
dimedone	5.6	6.0	−1.4
	(6.3)	(6.6)	(−1.3)
	[2.9]	[3.3]	[−1.2]
cyclopentanedione	4.5	5.2	−2.5
indanedione	14.7	14.6	0.3
cyclic-CONHR amides			
Meldrum acid *N*-Ph (MA-*N*-Ph)	−11.6	−10.3	−4.0
	(−9.6)	(−9.3)	(−3.6)
	[−13.4]	[−12.3]	[−3.8]
	−9.9^d	−8.5^d	−4.4^d
	(−7.6)^d	(−7.3)^d	(−4.3)^d
	[−12.0]^d	[−10.8]^d	[−4.3]^d
Meldrum acid *N*-C_6H_4Br-*p*	−11.0	−9.6	−4.8
	−9.7^d	−8.3^d	−4.8^d
Meldrum acid *N*-Pr-*i* (MA-*N*-Pr-*i*)	−12.5	−10.5	−6.6
	(−12.9)	(−10.7)	(−7.2)
	[−16.6]	[−14.8]	[−6.0]
	−15.0^d	−12.8^d	−7.2^d
dimedone *N*-Ph (DIM-*N*-Ph)	−14.0	−11.9	−7.1
	−15.0^d	−12.7^d	−7.7^d
cyclopentanedione *N*-Ph (CPD-*N*-Ph)	−14.9	−14.0	−3.3
	−17.0^d	−15.5^d	−5.3^d
indanedione-*N*-Ph (IND-*N*-Ph)	−8.3	−7.0	−4.4
	−7.9^d	−6.5^d	−4.8^d

[a] $\Delta H°$ and $\Delta G°$ are in kcal mol^{-1}, and $\Delta S°$ is in cal mol^{-1} K^{-1}. [b] Data for the (*E*)-enol form. [c] Data for the (*Z*)-enol form. [d] For the enol form on the carbonyl group.

mation. The order of the charges for the three species is strongly system-dependent.

For the CH_2YY' systems, the C−H carbon is negative and the C=O and C≡N carbons are positive. For the diesters and the $(CN)CO_2CH_2CF_3$ (R′ = CF_3 excluded) derivatives, the oxygen is more negative in order A: enol > anion > CH_2YY'. Order B (anion > enol > CH_2YY') applies for all other systems and $(CO_2CH_3)CO_2CH_2CF_3$. C-3 is more negative in order C (CH_2YY' > anion > enol) for the diesters and the cyclic systems, except IND, but order D (anion > CH_2YY' > enol) applies for the cyano-substituted systems and IND. C-2 is always more positive for CH_2YY', except for $(CN)_2$. C-4 is more positive in the diesters and the cyclic CH_2YY' and in the enol than in the anion. The cyanoesters obey order D.

In the trisubstituted systems, the heteroatoms and C_β are negative and other carbons are positive. The nitrogen is more negative in order E: anion > amide > enol. Order F (anion > enol > amide) applies for O-9 (N-9) and for O-7 (N-7) of the *N*-Pr-*i* derivatives except for $(CO_2CH_2CF_3)_2$. Order G (enol > anion > amide) applies for O-7 and O-8 and for the *N*-Ph derivatives, but for $(CN)_2$ it is amide > enol. C-4 follows order H: amide > anion > enol. The positive charge in C-3 follows the order: amide > enol ∼ anion ($(CN)_2$ excluded). For C-5 and C-6, order H applies except for C-6 of CPD-*N*-Ph, and anion > enol for the cyanoesters.

Enol/Enolate Geometry and Charge Comparisons. Our assumption that the enol is highly dipolar predicts that its C_β atom should be close in geometry and charge distribution to the enolate ion. The data in Tables 4 and 5 and S1−S3 enable this assumption to be probed.

In the open-chain compounds, the C_α−C_β bond lengths in the anion are 1.465 ± 0.005 and 1.471 ± 0.007 Å for all the *N*-Ph and *N*-Pr-*i* systems, respectively. The largest deviation is for the $(CN)_2$ compounds where the bond lengths are 0.015 (*N*-Ph) and 0.017 Å (*N*-Pr-*i*) shorter than the averages of 1.467 ± 0.04 and 1.473 ± 0.04 Å for other $(CN)_2$ derivatives.

In the enols, the average of all the C=C bond lengths are 1.427 ± 0.014 (*N*-Ph) and 1.428 ± 0.015 (*N*-Pr-*i*)Å [1.443 ± 0.02 (six diesters), 1.419 ± 0.02 (six cyanoesters), 1.404 ± 0.005 (two dicyano derivatives)]. The $\Delta(d(\text{anion}) - d(\text{enol}))$ values increase from 0.023 ± 0.003 (*N*-Ph) and 0.030 ± 0.002 (*N*-Pr-*i*) for CO_2R and CO_2R' to 0.049 ± 0.001 (*N*-Ph) and 0.053 ± 0.001 (*N*-Pr-*i*) Å for CN and Y

TABLE 4. Bond Lengths of Optimized Structures at B3LYP/6-31+G*//B3LYP/6-31+G*, B3LYP/6-311+G*//B3LYP/6-311+G* (in Parentheses), and B3LYP/6-311+G//B3LYP/6-311+G** (in Brackets) for Anion, Enol, and Amide Forms of *N*-Ph and *N*-Pr-*i* Noncyclic Systems (in Å)**

YY′ in species	N2H1	RN2	N2C3	C3O7	O7H10	C3C4	C4C5	C4C6	C5O9	C6O8	C5N9	C6N8	O8H10	O9H1	N9H1	N2O9	O7O8
anion PhNHCOCYY′⁻																	
$(CO_2Me)_2$	1.024	1.386	1.404	1.242		1.459	1.420	1.476	1.253	1.220				1.805		2.688	3.007
$(CO_2Me)CO_2CH_2CF_3$[a]	1.023	1.389	1.400	1.239		1.469	1.429	1.461	1.250	1.219				1.794		2.676	2.900
$(CO_2CH_2CF_3)_2$	1.021	1.391	1.398	1.238		1.470	1.415	1.467	1.246	1.217				1.825		2.697	2.943
$(CN)CO_2Me$	1.023	1.389	1.400	1.240		1.464	1.428	1.419	1.249			1.170		1.823		2.703	
$(CN)CO_2CH_2CF_3$	1.022	1.391	1.396	1.238		1.468	1.419	1.420	1.247			1.169		1.839		2.713	
$(CN)CO_2CH(CF_3)_2$	1.020	1.394	1.394	1.237		1.473	1.410	1.421	1.242			1.168		1.860		2.726	
$(CN)_2$	1.013	1.392	1.410	1.238		1.452	1.409	1.413			1.172	1.176			2.662		
anion *i*-PrNHCOCYY′⁻																	
$(CO_2Me)_2$	1.020	1.452	1.389	1.247		1.468	1.420	1.469	1.252	1.222				1.865		2.711	2.986
	(1.016)	(1.451)	(1.389)	(1.240)		(1.465)	(1.417)	(1.469)	(1.245)	(1.215)				(1.879)		(2.716)	(2.998)
	[1.018]	[1.451]	[1.388]	[1.240]		[1.465]	[1.416]	[1.469]	[1.245]	[1.215]				[1.864]		[2.706]	[2.998]
$(CO_2Me)CO_2CH_2CF_3$[a]	1.020	1.453	1.387	1.244		1.476	1.429	1.455	1.249	1.221				1.856		2.702	2.903
$(CO_2CH_2CF_3)_2$	1.017	1.455	1.380	1.244		1.477	1.414	1.461	1.245	1.219				1.888		2.717	2.942
$(CN)CO_2Me$	1.019	1.451	1.381	1.246		1.469	1.425	1.418	1.249			1.171		1.889	2.725		
	(1.015)	(1.450)	(1.381)	(1.239)		(1.468)	(1.422)	(1.414)	(1.242)			(1.163)		(1.898)	(2.725)		
	[1.017]	[1.450]	[1.380]	[1.239]		[1.468]	[1.422]	[1.414]	[1.242]			[1.163]		[1.884]	[2.717]		
$(CN)CO_2CH_2CF_3$	1.018	1.452	1.379	1.244		1.474	1.416	1.419	1.247			1.170		1.905	2.734		
$(CN)CO_2CH(CF_3)_2$	1.017	1.454	1.377	1.243		1.477	1.407	1.420	1.242			1.169		1.923	2.743		
$(CN)_2$	1.014	1.455	1.398	1.243		1.456	1.408	1.412			1.173	1.176			2.739		
	(1.010)	(1.454)	(1.397)	(1.236)		(1.454)	(1.408)	(1.404)			(1.164)	(1.168)			(2.735)		
	[1.011]	[1.454]	[1.397]	[1.236]		[1.454]	[1.408]	[1.404]			[1.164]	[1.168]			[2.730]		
enol PhNHC(OH)═CYY′																	
$(CO_2Me)_2$	1.028	1.414	1.341	1.317	1.025	1.441	1.462	1.454	1.241	1.254			1.508	1.731		2.610	2.460
$(CO_2Me)CO_2CH_2CF_3$[a]	1.026	1.416	1.340	1.315	1.026	1.443	1.454	1.457	1.239	1.253			1.505	1.751		2.622	2.459
$(CO_2CH_2CF_3)CO_2Me$[b]	1.029	1.416	1.380	1.318	1.018	1.442	1.466	1.447	1.240	1.252			1.532	1.732		2.612	2.473
$(CO_2CH_2CF_3)_2$	1.023	1.417	1.337	1.316	1.019	1.445	1.457	1.450	1.238	1.250			1.528	1.747		2.619	2.470
$(CN)CO_2Me$	1.015	1.418	1.349	1.318	1.016	1.416	1.416	1.444		1.247	1.168		1.598		2.709		2.532
$(CN)CO_2CH_2CF_3$	1.016	1.420	1.343	1.318	1.012	1.419	1.417	1.438		1.245	1.167		1.619		2.696		2.544
$(CN)CO_2CH(CF_3)_2$	1.016	1.421	1.343	1.318	1.007	1.422	1.417	1.431		1.240	1.167		1.641		2.687		2.557
$(CN)_2$	1.015	1.422	1.346	1.335	0.978	1.403	1.417	1.416			1.167	1.169	2.624		2.781		
enol *i*-PrNHC(OH)═CYY′																	
$(CO_2Me)_2$	1.023	1.470	1.332	1.323	1.020	1.441	1.460	1.452	1.240	1.254			1.529	1.793		2.624	2.474
	(1.019)	(1.470)	(1.329)	(1.321)	(1.007)	(1.438)	(1.460)	(1.452)	(1.233)	(1.246)			(1.559)	(1.800)		(2.621)	(2.481)
	[1.022]	[1.470]	[1.329]	[1.317]	[1.019]	[1.439]	[1.459]	[1.449]	[1.233]	[1.248]			[1.500]	[1.786]		[2.617]	[2.448]
$(CO_2Me)CO_2CH_2CF_3$[b]	1.022	1.472	1.331	1.321	1.020	1.443	1.452	1.455	1.238	1.252			1.529	1.809		2.634	2.473
$(CO_2CH_2CF_3)_2$	1.022	1.473	1.328	1.322	1.013	1.447	1.456	1.448	1.234	1.248			1.550	1.803		2.627	2.481
$(CN)CO_2Me$	1.015	1.474	1.339	1.323	1.013	1.417	1.416	1.442		1.248	1.168		1.614		2.784		2.543
	(1.011)	(1.473)	(1.336)	(1.320)	(1.000)	(1.413)	(1.412)	(1.442)		(1.239)	(1.160)		(1.648)		(2.778)		(2.554)
	[1.012]	[1.473]	[1.337]	[1.317]	[1.011]	[1.414]	[1.412]	[1.439]		[1.242]	[1.160]		[1.586]		[2.786]		[2.517]
$(CN)CO_2CH_2CF_3$	1.015	1.476	1.336	1.322	1.008	1.420	1.417	1.435		1.243	1.167		1.639		2.771		2.556
$(CN)CO_2CH(CF_3)_2$	1.015	1.476	1.334	1.322	1.005	1.423	1.417	1.429		1.240	1.167		1.657		2.764		2.567
$(CN)_2$	1.015	1.477	1.337	1.340	0.977	1.404	1.416	1.416			1.168	1.169	2.634		2.852		
	(1.012)	(1.476)	(1.335)	(1.336)	(0.971)	(1.400)	(1.412)	(1.412)			(1.159)	(1.161)	(2.646)		(2.851)		
	[1.012]	[1.476]	[1.335]	[1.336]	[0.970]	[1.400]	[1.413]	[1.412]			[1.159]	[1.161]	[2.636]		[2.844]		
amide PhNHCOCHYY′																	
$(CO_2Me)_2$	1.018	1.414	1.359	1.225		1.558	1.525	1.535	1.216	1.212				1.971		2.784	4.075
$(CO_2Me)CO_2CH_2CF_3$	1.020	1.417	1.351	1.231		1.557	1.529	1.548	1.216	1.206				1.908		2.757	4.015
$(CO_2CH_2CF_3)_2$	1.018	1.416	1.358	1.223		1.564	1.523	1.531	1.216	1.206				1.996		2.800	4.117
$(CN)CO_2Me$[c]	1.018	1.417	1.357	1.221		1.572	1.536	1.467	1.216			1.161		2.076		2.860	
$(CN)CO_2CH_2CF_3$[c]	1.016	1.418	1.357	1.220		1.576	1.532	1.467	1.211			1.161		2.194		2.925	
$(CN)CO_2CH(CF_3)_2$[d]	1.014	1.421	1.356	1.220		1.574	1.535	1.463		1.161	1.202				2.662	3.697	3.700
$(CN)_2$	1.014	1.422	1.356	1.217		1.583	1.470	1.472			1.160	1.160			2.702		
amide *i*-PrNHCOCHYY′																	
$(CO_2Me)_2$	1.016	1.469	1.351	1.228		1.552	1.524	1.534	1.218	1.210				2.203		2.936	3.200
	(1.012)	(1.468)	(1.349)	(1.220)		(1.551)	(1.523)	(1.533)	(1.210)	(1.202)				(2.204)		(2.931)	(3.570)
	[1.013]	[1.468]	[1.349]	[1.220]		[1.551]	[1.523]	[1.533]	[1.210]	[1.202]				[2.194]		[2.927]	[3.545]
$(CO_2Me)CO_2CH_2CF_3$[a]	1.016	1.469	1.347	1.228		1.556	1.529	1.529	1.216	1.206				2.093		2.860	3.637
$(CO_2CH_2CF_3)_2$	1.016	1.471	1.352	1.224		1.563	1.521	1.529	1.212	1.209				2.147		2.869	4.389
$(CN)CO_2Me$[c]	1.016	1.471	1.348	1.224		1.572	1.535	1.467	1.215			1.161		2.159		2.900	
	(1.013)	(1.471)	(1.347)	(1.216)		(1.573)	(1.535)	(1.461)	(1.207)			(1.153)		(2.180)		(2.908)	
	[1.013]	[1.471]	[1.347]	[1.216]		[1.573]	[1.535]	[1.461]	[1.207]			[1.153]		[2.166]		[2.902]	
$(CN)CO_2CH_2CF_3$[c]	1.015	1.473	1.348	1.222		1.577	1.530	1.466	1.210			1.161		2.300		2.985	
$(CN)CO_2CH(CF_3)_2$[c]	1.015	1.473	1.348	1.222		1.577	1.530	1.466	1.210			1.161		2.300		3.039	
$(CN)_2$	1.014	1.475	1.347	1.222		1.582	1.470	1.472		1.160	1.161				2.755		
	(1.011)	(1.475)	(1.345)	(1.212)		(1.583)	(1.465)	(1.460)		(1.152)	(1.153)				(2.764)		
	[1.010]	[1.475]	[1.345]	[1.212]		[1.583]	[1.464]	[1.466]		[1.151]	[1.153]				[2.748]		

[a] R^1 = Me, R^2 = CH_2CF_3. [b] R^1 = CH_2CF_3, R^2 = Me. [c] Amide B. [d] Amide C.

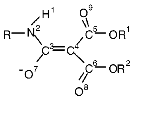

Anion A

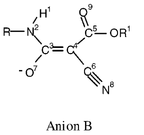

Anion B

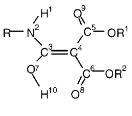

Enol A

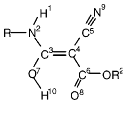

Enol B

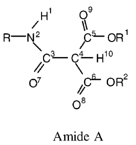

Amide A

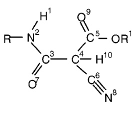

Amide B

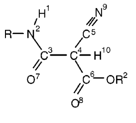

Amide C

[R = Ph or *i*-Pr]

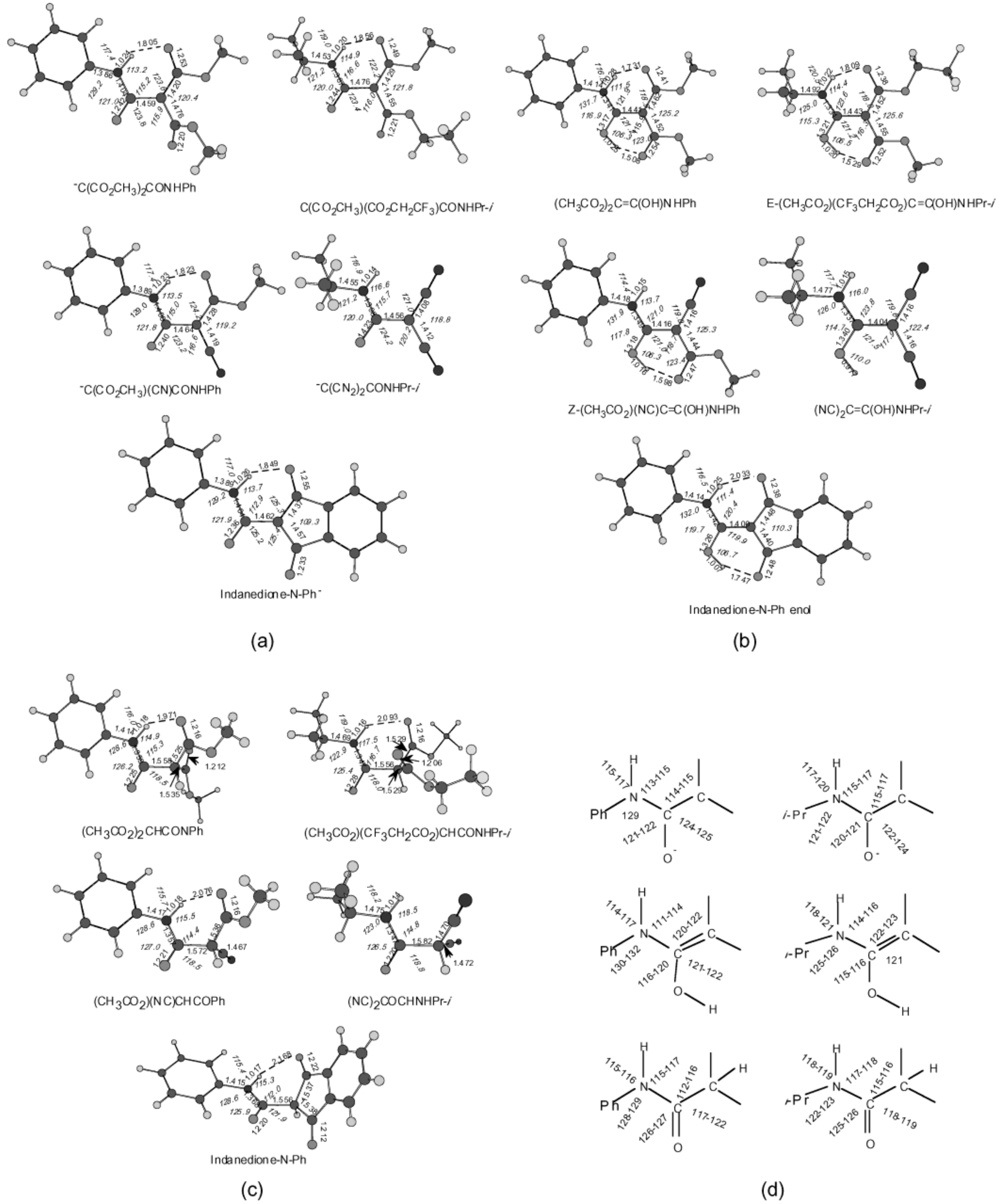

FIGURE 11. B3LYP/6-31G*-calculated bond lengths in selected structure of (a) anions, (b) enols, and (c) amides. (d) Ranges of angles for anions, enols, and amides of *N*-Ph-substituted systems.

(Y = CN, CO$_2$R). The C=O group in the diesters that is hydrogen bonded to the O−H is somewhat longer than the other.

The corresponding natural charges are positive at C$_\alpha$ and negative at C$_\beta$. In the anion, they are 0.668 ± 0.003 (*N*-Ph) and 0.667 ± 0.002 (*N*-Pr-*i*) at C$_\alpha$ with the smallest

TABLE 5. Natural Charges at B3LYP/6-31+G*//B3LYP/6-31+G*, B3LYP/6-311+G*//B3LYP/6-311+G* (in Parentheses), and B3LYP/6-311+G//B3LYP/6-311+G** (in Brackets) of Anion, Enol, and Amide Forms of *N*-Ph and *N*-Pr-*i* Noncyclic Systems**[a]

species: YY′	H1	N2	C3	C4	C5	C6	O7	O8	O9	N8	N9	H10
anion $PhNHCOCYY'^-$												
$(CO_2Me)_2$	0.454	−0.656	0.662	−0.474	0.753	0.828	−0.690	−0.627	−0.740			
$(CO_2CH_3)CO_2CH_2CF_3$[b]	0.454	−0.656	0.668	−0.479	0.765	0.814	−0.679	−0.621	−0.729			
$(CO_2CH_2CF_3)_2$	0.453	−0.653	0.670	−0.471	0.756	0.823	−0.674	−0.610	−0.721			
$(CN)CO_2CH_3$	0.454	−0.656	0.667	−0.492	0.765	0.327	−0.681		−0.729	−0.444		
$(CN)CO_2CH_2CF_3$	0.453	−0.654	0.670	−0.483	0.757	0.321	−0.673		−0.724	−0.425		
$(CN)CO_2CH(CF_3)_2$	0.453	0.651	0.674	−0.476	0.754	0.319	−0.666		−0.710	−0.413		
$(CN)_2$	0.432	−0.646	0.664	−0.531	0.284	0.322	−0.678			−0.440	−0.460	
anion *i*-$PrNHCOCYY'^-$												
$(CO_2Me)_2$	0.444	−0.711	0.664	−0.481	0.752	0.821	−0.714	−0.637	−0.744			
	(0.414)	(−0.687)	(0.668)	(−0.478)	(0.755)	(0.824)	(−0.716)	(−0.632)	(−0.748)			
	[0.419]	[−0.694]	[0.667]	[−0.477]	[0.755]	[0.823]	[−0.716]	[−0.632]	[−0.748]			
$(CO_2CH_3)CO_2CH_2CF_3$[b]	0.444	−0.708	0.668	−0.483	0.763	0.807	−0.703	−0.631	−0.733			
$(CO_2CH_2CF_3)_2$	0.447	−0.707	0.669	−0.474	0.753	0.817	−0.700	−0.618	−0.725			
$(CN)CO_2CH_3$	0.447	−0.707	0.666	−0.497	0.760	0.331	−0.712	−0.735			−0.460	
	(0.417)	(−0.684)	(0.670)	(−0.498)	(0.763)	(0.339)	(−0.711)	(−0.738)			(−0.466)	
	[0.422]	[−0.690]	[0.669]	[−0.498]	[0.764]	[0.339]	[−0.711]	[−0.738]			[−0.466]	
$(CN)CO_2CH_2CF_3$	0.446	−0.703	0.668	−0.487	0.752	0.325	−0.702	−0.730			−0.439	
$(CN)CO_2CH(CF_3)_2$	0.456	−0.698	0.671	−0.478	0.749	0.323	−0.695	−0.714			−0.426	
$(CN)_2$	0.419	−0.703	0.663	−0.541	0.292	0.325	−0.701			−0.458	−0.477	
	(0.384)	(−0.678)	(0.668)	(−0.549)	(0.303)	(0.334)	(−0.702)			(−0.464)	(−0.485)	
	[0.386]	[−0.684]	[0.668]	[−0.549]	[0.303]	[0.334]	[−0.702]			[−0.464]	[−0.485]	
enol $PhNHC(OH){=}CYY'$												
$(CO_2Me)_2$	0.474	−0.597	0.667	−0.438	0.804	0.806	−0.702	−0.700	−0.686			0.546
$(CO_2CH_3)CO_2CH_2CF_3$[c]	0.473	−0.594	0.670	−0.438	0.802	0.810	−0.698	−0.695	−0.680			0.546
$(CO_2CH_2CF_3)_2$	0.474	−0.590	0.672	−0.436	0.812	0.805	−0.695	−0.691	−0.675			0.547
$(CN)CO_2CH_3$	0.453	−0.587	0.662	−0.450	0.270	0.807	−0.694	−0.687			−0.345	0.551
$(CN)CO_2CH_2CF_3$	0.455	−0.582	0.665	−0.448	0.266	0.803	−0.689	−0.683			−0.332	0.552
$(CN)CO_2CH(CF_3)_2$	0.460	−0.578	0.669	−0.446	0.265	0.805	−0.685	−0.672			−0.325	0.553
$(CN)_2$	0.454	−0.586	0.642	−0.454	0.269	0.257	−0.674			−0.326	−0.325	0.542
enol *i*-$PrNHC(OH){=}CYY'$												
$(CO_2Me)_2$	0.471	−0.623	0.668	−0.447	0.802	0.804	−0.710	−0.705	−0.689			0.544
	(0.440)	(−0.597)	(0.672)	(−0.439)	(0.798)	(0.801)	(−0.672)	(−0.704)	(−0.690)			(0.506)
	[0.445]	[−0.604]	[0.673]	[−0.438]	[0.799]	[0.802]	[−0.678]	[−0.702]	[−0.690]			[0.506]
$(CO_2CH_3)CO_2CH_2CF_3$[c]	0.470	−0.619	0.671	−0.446	0.800	0.808	−0.706	−0.698	−0.683			0.545
$(CO_2CH_2CF_3)_2$	0.471	−0.613	0.675	−0.444	0.808	0.809	−0.701	−0.691	−0.674			0.546
$(CN)CO_2CH_3$	0.448	−0.619	0.665	−0.462	0.277	0.805	−0.701	−0.692			−0.356	0.549
	(0.412)	(−0.591)	(0.671)	(−0.464)	(0.284)	(0.803)	(−0.663)	(−0.693)			(−0.362)	(0.513)
	[0.416]	[−0.598]	[0.672]	[−0.463]	[0.284]	[0.805]	[−0.669]	[−0.692]			[−0.362]	[0.514]
$(CN)CO_2CH_2CF_3$	0.450	−0.613	0.670	−0.459	0.274	0.805	−0.696	−0.684			0.344	−0.550
$(CN)CO_2CH(CF_3)_2$	0.451	−0.609	0.672	−0.455	0.271	0.803	−0.692	−0.676			0.334	−0.551
$(CN)_2$	0.451	−0.618	0.650	−0.470	0.258	0.273	−0.686			−0.335	−0.335	0.542
	[0.418]	[−0.597]	[0.660]	[−0.476]	[0.266]	[0.280]	[−0.657]			[−0.342]	[−0.339]	[0.511]
amide $PhNHCOCHYY'$												
$(CO_2Me)_2$	0.458	−0.627	0.688	−0.504	0.839	0.826	−0.612	−0.594	−0.609			0.319
$(CO_2CH_3)CO_2CH_2CF_3$[b]	0.460	−0.618	0.688	−0.517	0.847	0.840	−0.639	−0.552	−0.606			0.298
$(CO_2CH_2CF_3)_2$	0.455	−0.627	0.686	−0.507	0.843	0.829	−0.595	−0.583	−0.595			0.327
$(CN)CO_2CH_3$[d]	0.454	−0.626	0.695	−0.508	0.836	0.279	−0.596		−0.607	−0.286		0.334
$(CN)CO_2CH_2CF_3$[d]	0.451	−0.623	0.696	−0.509	0.841	0.274	−0.589		−0.590	−0.276		0.336
$(CN)CO_2CH(CF_3)_2$[e]	0.446	−0.613	0.697	−0.511	0.265	0.848	−0.595	−0.552		−0.278		0.337
$(CN)_2$	0.444	−0.615	0.702	−0.515	0.266	0.283	−0.586			−0.260	−0.270	0.350
amide *i*-$PrNHCOCHYY'$												
$(CO_2Me)_2$	0.444	−0.654	0.695	−0.503	0.828	0.833	−0.632	−0.583	−0.617			0.317
	(0.410)	(−0.631)	(0.699)	(−0.461)	(0.827)	(0.833)	(−0.630)	(−0.579)	(−0.616)			(0.271)
	[0.414]	[−0.637]	[0.700]	[−0.464]	[0.828]	[0.834]	[−0.629]	[−0.578]	[−0.617]			[0.273]
$(CO_2CH_3)CO_2CH_2CF_3$[b]	0.449	−0.654	0.691	−0.501	0.827	0.836	−0.633	−0.570	−0.609			0.319
$(CO_2CH_2CF_3)_2$	0.447	−0.659	0.688	−0.508	0.834	0.843	−0.612	−0.594	−0.581			0.325
$(CN)CO_2CH_3$[d]	0.448	−0.658	0.694	−0.508	0.835	0.283	−0.614		−0.606	−0.290		0.332
	(0.414)	(−0.633)	(0.701)	(−0.469)	(0.833)	(0.294)	(−0.611)		(−0.603)	(−0.303)		(0.285)
	[0.418]	[−0.639]	[0.701]	[−0.472]	[0.834]	[0.295]	[−0.611]		[−0.603]	[−0.303]		[0.287]
$(CN)CO_2CH_2CF_3$[d]	0.445	−0.656	0.695	−0.509	0.839	0.279	−0.606		−0.589	−0.284		0.335
$(CN)CO_2CH(CF_3)_2$[d]	0.443	−0.654	0.696	−0.510	0.841	0.276	−0.598		−0.572	−0.279		0.338
$(CN)_2$	0.439	−0.649	0.702	−0.516	0.271	0.286	−0.603			−0.266	−0.276	0.348
	(0.403)	(−0.623)	(0.708)	(−0.473)	(0.281)	(0.296)	(−0.600)			(−0.274)	(−0.284)	(0.300)
	[0.408]	[−0.630]	[0.708]	[−0.482]	[0.282]	[0.297]	[−0.600]			[−0.274]	[−0.284]	[0.301]

[a] For numbering of atoms, see Table 4. [b] $R^1 = Me$, $R^2 = CH_2CF_3$ (cf. Table 4). [c] $R^1 = CH_2CF_3$, $R^2 = Me$ (cf. Table 4). [d] Amide B (cf. Table 4). [e] Amide C (cf. Table 4).

value for $(CN)_2$. At C_β, they are −0.479 ± 0.006 (*N*-Ph), −0.483 ± 0.006 (*N*-Pr-*i*) for all compounds except $(CN)_2$, with the highest value for $CN(CO_2Me)$. The different values of −0.531 and −0.541 for the $(CN)_2$ derivatives

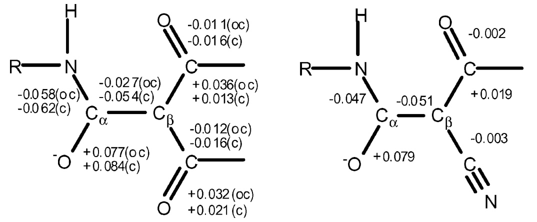

FIGURE 12. Average changes in bond lengths $\Delta[d(\text{anion}) - d(\text{enol})]$ in Å occurring on ionization of the enolic hydrogen of (A) β-dicarbonyl (c = cyclic; oc = open chain) systems and (B) β-carbonyl-β-cyano-substituted systems.

are significant. In the enols, the values are 0.667 ± 0.03 (*N*-Ph), 0.670 ± 0.03 (*N*-Pr-*i*), 0.642 (*N*-Ph, $(CN)_2$), and 0.650 (*N*-Pr-*i*, $CN)_2$) at C_α and −0.443 ± 0.006 (*N*-Ph), −0.453 ± 0.006 (*N*-Pr-*i*), and −0.454 and −0.470 for the $(CN)_2$ derivatives.

The charges at C_α differ between the two species by $|0.001| - |0.006|$, except for 0.022 and 0.013 for the $(CN)_2$ derivatives. At C_β, the differences are greater, being between −0.023 and −0.045 (−0.077 and −0.071 for the $(CN)_2$ derivatives). Consequently, C_β is less negative in the enol, and the effect is most pronounced in the $(CN)_2$ compounds.

For the N−R cyclic derivatives the C−O bond lengths are 1.236 ± 0.002 (anion) and 1.320 ± 0.004 Å (enol), and the corresponding C−N bond lengths are 1.398 ± 0.006 and 1.336 ± 0.003 Å, respectively. The two C_β−C═O bonds are 1.432 ± 0.002 and 1.452 ± 0.005 (cis to O) Å in the ion and 1.445 ± 0.004 and 1.446 ± 0.010 Å in the enol, respectively. The C−C bond lengths in the ions and the enols are 1.477 ± 0.010 and 1.423 ± 0.013 Å, respectively.

The changes in the important bond lengths occurring on ionization are shown schematically in Figure 12. The C═C and the C−N bonds elongate, and the C−O bonds shorten appreciably. The two C_β−EWG bonds are less affected: the bond cis to the oxygen elongates and the bond trans to the oxygen shortens on ionization. The C═O bond involved in the O−H···O═ hydrogen bond elongates, and the one involved in the N−H···O═ hydrogen bond shortens on ionization.

Amide/Enolate Geometry and Charge Distribution. The long CO−C_β bonds in the amides are shortened by 0.08−0.13 Å in the anions. The shortening increases in the order diesters < cyanoesters < $(CN)_2$. The change and the differential change for the $(CN)_2$ compounds are the largest. The corresponding changes in the natural charges are larger positive charges of the amide carbonyl carbon by 0.016−0.039, with the largest values for the $(CN)_2$ derivatives. The charges on C_β are more negative in the amide by 0.018−0.038, except that for the $(CN)_2$ derivatives they are less negative by 0.016−0.030.

Discussion

Deprotonation Site. There are three potential deprotonation sites for our amides/enols: the C_β−H bond of the amide and the enolic O−H and the N−H of either the amide or the enol form. Kass et al.[8a] investigated by mass spectrometry, an afterglow method and computationally the anions derived from acetamide. The C-deprotonated enolate ($^-CH_2CONH_2 \leftrightarrow CH_2{=}C(O^-)NH_2$) was found to have a higher proton affinity (373 ± 3 kcal/mol)[8a] than the N-deprotonated amidate ion ($CH_3CONH^- \leftrightarrow CH_3C(O^-){=}NH$; 362.1 ± 2.1 kcal/mol).[8c,10] Hence, ionization at the NH site is favored by 11.4 kcal/mol, although computations give higher differences. The interconversion of the ions have a high activation barrier (>32 kcal/mol, obsd; 36.4−39.2 kcal/mol, calcd). Hence, the NH proton in our system is a potential deprotonation site, and although $\Delta G°_{\text{acid}}(PhNH_2)$ = 359.1 kcal/mol[10] is a much higher value than that for our compounds, the EWGs Y,Y′ could have brought the acidity to the observed range. Two lines of evidence are against this assumption. First, $\Delta G°_{\text{acid}}(p\text{-}ClC_6H_4NH_2)$ of 353.1 kcal/mol[10] should resemble $\Delta G°_{\text{acid}}(p\text{-}BrC_6H_4NH_2)$ due to the similar electronic effects of the two halogens judging by their various σ values.[14] The 6 kcal/mol effect of *p*-Br on ionization from the NH group is much higher than the effect of 1.0−2.0 kcal/mol of *p*-Br in our systems, despite the similar aniline-type moiety. Second, the relative stabilities of the anions formed by deprotonation of C_β (taken as 0.0 kcal/mol) and the nitrogen were calculated for the $RNHCOCH(CO_2Me)_2$ system. The relative energies of the latter ions at B3LYP/6-31+G* are 17.1 (R = Ph) and 19.7 (R = *i*-Pr) kcal/mol, indicating a preferred ionization at C_β .

The shift of >30 kcal/mol in the preference for a C−H vs N−H ionization site caused by β,β-EWG substitution is not surprising. The enolate ion benefits from negative charge delocalization by both the oxygen (cf. **3**) and the $C_\beta YY'$ moieties (cf. **4**−**6** in eq 4) as compared with that by the oxygen and the nitrogen in the amidate ion, and the effect of the Y and Y′ groups on the latter ionization is only inductive.

The question if the ionization site is the amide C_β−H or the enol OH still remains. Most compounds studied exist in the solid as the enols, except for the CO_2Me and CO_2R derivatives, R = Me, CH_2CF_3, which in the solid are the amides,[6c] and perhaps the CN,CN species whose solid-state structure is unknown. However, the structure of the solid compound introduced into the ICR spectrometer is not necessarily that of the ionized species since isomerization may take place on raising the temperature.

The situation differs from that for the ionization of the ketone Ar_2CHCOR/enol $Ar_2C{=}C(OH)R$ pairs,[9] which were available as different solid entities, and each member of the isomeric pair gave a different $\Delta G_{\text{acid}}°$ value. Moreover, the ketones and the enols gave different correlations, excluding isomerization of the neutral during the ICR experiment. In the present case there is only one solid species for each pair, and the diesters that exist in the solid either as amides or enols obey the same correlations (e.g., cf. Figures 1 and 3−6).

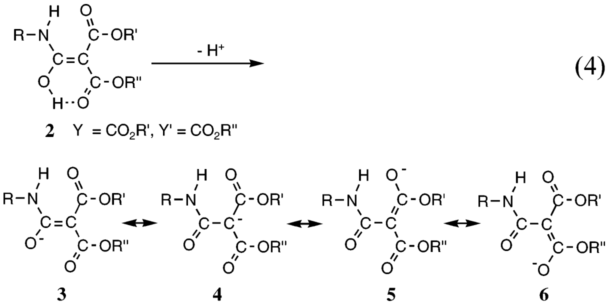

(4)

2 Y = CO_2R', Y' = CO_2R''

3 **4** **5** **6**

The calculations were partially conducted in order to answer this question. The plots in Figures 3−5 suggest that the ionizing species is the enol, except for the CO_2Me, CO_2R (R = Me), and CH_2CF_3 systems, where the ionization site cannot be deduced since calculations for the amide and the enol gave sufficiently close values. However, at B3LYP/6-311++G**//B3LYP/6-311++G**, the calculated value for the enol *i*-PrNHC(OH)═C(CO_2Me)$_2$ is only 0.2 kcal/mol lower than the experimental value, whereas the $\Delta G°_{acid}$ value for the amide *i*-PrNHCOCH(CO_2Me)$_2$ ionization is 3.1 kcal/mol lower than the experimental value. On this basis, the $(CO_2Me)_2$ system and, by extrapolation, also the $CO_2Me(CO_2CH_2CF_3)$ systems, which are more enolic in solution,[6c] ionize as enols, as do the other compounds.

For the $(CN)_2$ compounds, the ionization site seems to be the amide C−H on the basis of the better fit of the points for the amides to the plot. This is not surprising since the $(CN)_2$-substituted enols are unique among our enols by lacking intramolecular hydrogen bonding stabilization due to the linearity of the enol sp^2 geometry. However, the calculation at B3LYP/6-311+G**//B3LYP/6-311+G** level for the *i*-PrNHCOCH$(CN)_2$ system reduces the 4.3 kcal/mol gap in favor of the amide ionization to only 1.1 kcal/mol. The values are still 5.3−6.4 kcal/mol lower than the experimental value. Consequently, a definite conclusion concerning the enolization site is not achieved.

Acidity as a Function of the N-Substituent. All the compounds in the *N*-Ph series are 6−8 kcal/mol stronger acids, both experimentally and computationally, than their *N*-Pr-*i* analogues. This is ascribed to inductive electron withdrawal by the Ph and the *p*-BrC_6H_4 groups compared with the inductive electron-donating *i*-Pr. The effect is larger than that for the $RCOCH_2COMe$ system ($\Delta G°_{acid}$ = 333.0 (R = Ph), 336.7 (R = Me))[13] despite the direct resonance interaction with the phenyl group in the enolate anion of the diketone.

The good linearity between either the observed or the calculated $\Delta G°_{acid}$ values for the *N*-Pr-*i* and the *N*-Ph series (Figure 1) supports the conclusion that the ionizing species is the enol. A similar plot using the calculated values for the amides of the CF_3-substituted diesters shows deviation from linearity.

The deviation of the point for Meldrum's acid from Figure 1 can be due either to a calculated 3 kcal/mol stronger acidity for the Ph derivative or to a 3 kcal/mol weaker acidity of the *N*-Pr-*i* compound.

Acidity as a Function of Y and Y′. The effect of Y and Y′ on the acidity of the three systems is shown in Figure 2. The change $CO_2Me \rightarrow CO_2CH_2CF_3$ increases the acidity additively by 8.5 ± 0.8, 6.35 ± 0.15, and 6.85 ± 0.05 kcal/mol for systems A, B, and C, respectively. The $CO_2Me \rightarrow CN$ change was additive (6.5 ± 0.3 kcal/mol) for $CH_2(CO_2Me)_2$ but showed a much larger effect for the first replacement in systems B and C. Interestingly, the successive change $CO_2CH_2CF_3 \rightarrow CN$ reduces the acidity of $CH_2(CO_2CH_2CF_3)_2$ by 0.5 and 3.6 kcal/mol but increases the acidity of the corresponding *i*-Pr and Ph enols by 7.5 ± 0.1 and 8.5 ± 0.15 kcal/mol, respectively. Likewise, the same change reduces the acidity of $CH_2(CO_2Me)CO_2CH_2CF_3$ by 1.0 kcal/mol but increases it by 8.35 ± 0.55 kcal/mol for the two enols. In the CN(CO_2Me) system, the change $CO_2Me \rightarrow CO_2CH_2CF_3$ is acid-strengthening by a similar value, as is the replacement in the $CO_2Me(CO_2CH_2CF_3)$ moieties of systems A−C.

Consequently, we see two acidifying orders by Y,Y′. For CH_2YY', the order is CO_2Me < CN < $CO_2CH_2CF_3$ < $CO_2CH(CF_3)_2$. For the two enols, the order is CO_2Me < $CO_2CH_2CF_3$ < CN, $CO_2CH(CF_3)_2$. We ascribe the different orders to a combination of polar and steric effects. The change in the number of fluorine atoms in the ester groups from 0 to 3 to 6 increases the acidity mainly by increasing the polar effect, while the steric effect is small since the change is at a remote position from the reaction center.

In the $^-CHYY'$ carbanion derived from CH_2YY', the steric interaction between the substituents is small and enables planarity to be achieved, and the $CO_2CH_2CF_3$ group can exert its full resonance delocalization ability. The planarity is corroborated by B3LYP/6-31+G* calculations for the $^-CH(CN)_2$ and $^-CH(CN)CO_2Me$ anions. In contrast, in the anion derived from the amide/enol−$(CO_2R)CO_2R'$ systems, the formal carbanionic C_β is trisubstituted, and complete planarity of the CO_2R, CO_2R', CONHR groups cannot be achieved. Consequently, at least one ester group does not exert its full delcoalization ability in the anion. When one CO_2R group is replaced by the sterically less demanding CN, the anion should become planar with a consequent higher stability and a stronger conjugate acid. This is again corroborated by B3LYP/6-31+G* calculations, which show that all the cyano anions are planar with <3° deviation of each group from the anion plane (Figure 13a). In contrast, the diester carbamido systems are severely twisted. The angle between the plane including the planar enolate moiety and one ester group and the plane of the second ester group is 40−54° for the six systems studied (Figure 13b). The differences in the geometries calculated at the three levels are small.

It could be argued that the parent enol that carries essentially the same groups plus the small hydrogen should be as twisted as the ion, but the calculation shows that the enol is planar, whereas the anion is not (Figure 13c). This reflects the strong hydrogen bond between the OH and the ester group cis to it in the enol, which leads to planarization. In contrast, repulsion between the negatively charged oxygens of the enolate anion and the *cis*-CO_2R C═O dipole results in a twist of this ester group from the enolate plane. When Y and Y′ are different ester groups, e.g., CO_2Me and $CO_2CH_2CF_3$, it is experimentally known that both in the solid state and in solution the hydrogen bond in the enol is stronger to the CO_2Me group than to the $CO_2CH_2CF_3$ group.[6c] The calculations also show that in the $CO_2Me(CO_2CH_2CF_3)$ anions, the $CO_2CH_2CF_3$ is the twisted group in the more stable anion and the CO_2Me is the twisted group in the less stable anion since the CO_2Me forms a stronger hydrogen bond to the N−H group than to the $CO_2CH_2CF_3$ group (Figure 13b).

The higher acidifying effect of a cyano compared with bulkier electron-withdrawing groups in an already crowded system is reflected in the additivity of the effect of the

---

(14) Lowry, T. H.; Richardson, K. S. *Mechanism and Theory in Organic Chemistry*, 3rd ed.; Harper and Row: New York, 1987; pp 144, 154, 157.

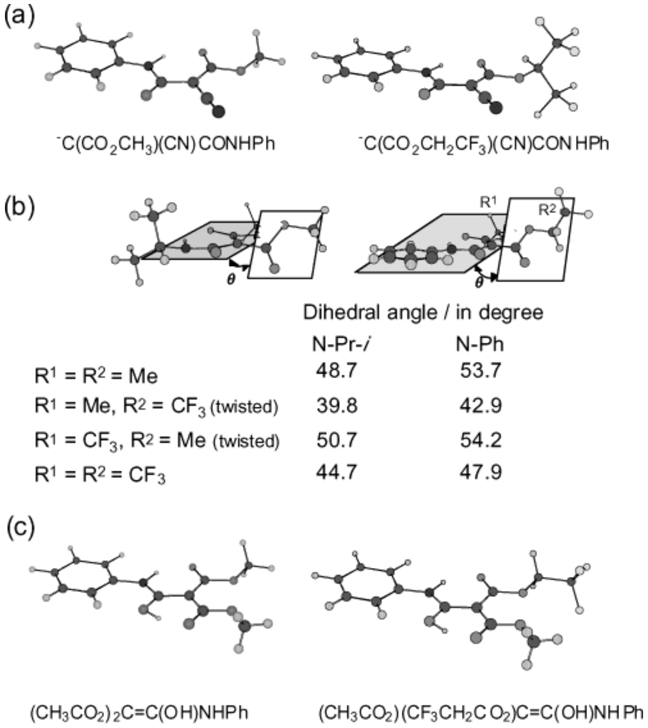

FIGURE 13. (a) Planarity of two cyano anions derived from $CH(CO_2R)(CONHPh)CN$ (R = Me or CH_2CF_3). (b) Distortions from planarity in the $^{-}C(CO_2Me)(CO_2R)CONHPh$ (R = Me, CH_2CF_3) anions. The $CO_2CH_2CF_3$ group is twisted in the more stable isomer where the CO_2Me is hydrogen bonded to the NH. The CO_2Me group is twisted in the less stable isomer where the $CO_2CH_2CF_3$ group is hydrogen bonded to the NH. The numbers given are values of θ, the twist angle of the CO_2R group from the anion plane. (c) The planar structure of the enols $(MeO_2C)(RO_2C)C{=}C(OH)NHPh$ (R = Me or CH_2CF_3) correspond to the anions in b above. All structures were calculated at the B3LYP/6-31+G* level.

CN group on gas-phase $\Delta G°_{acid}$ values, while other groups show a saturation effect. For the changes $CH_4 \rightarrow CH_3X \rightarrow CH_2X_2 \rightarrow CHX_3$, the consecutive $\Delta G°_{acid}$ values in kcal/mol are 44.5, 35.7, 34.8 (X = CN), 44.6, 25.2, 7.8 (X = COMe), 43.4, 23.8, 7.8 (X = CO_2Me), 66.4, 31.8, 9.7 (X = $COCF_3$), and 68.7, 38.5, and 10.3 (X = SO_2CF_3).[11,13]

The present work, which adds several gas-phase $\Delta G°_{acid}$ values for CH_2YY' systems, enables extension of a $\Delta G°_{acid}$(DMSO) vs $\Delta G°_{acid}$ (gas-phase) correlation for CH_2YY' carbon acids.[12,13] Figure 9 shows a linearity for gas-phase $\Delta G°_{acid}$ values of 350−325 kcal/mol and a plateau for fluorinated species. Since $\Delta G°_{acid}$ (DMSO) values for several of our systems are lacking, we cannot determine the point of break in the correlation.

Discrepancy between Meldrum's Acid and 1,3-Indanedione. Several of the correlations separate from linear correlations for the open-chain diesters and the cyanoesters, i.e., a single linear correlation comprised of all compounds is not realized. More pronounced steric effects in the diester-substituted enols than in the cyano ester-substituted enols and more so than in CH_2YY' seems an insufficient explanation, and additional effects should also be considered. For *N*-Ph-CPD and *N*-Ph-DIM[6a] systems, we believe that as in the solid, enolization in solution is on a ring carbonyl rather than on the amido carbonyl and do not expect them to be on the same correlation line. This is not the case for the *N*-Ph-MA and *N*-Ph-IND derivatives, whose positions in Figure 3a are apparently inverted, that for MA being on the diketone line, and that for the IND on the diester line. However, the IND derivative is an enol on the amido group in the solid.[11] If this also applies in the gas-phase, it resembles more the enols of β-diesters than of the β-diketones, although the fit to the diester line may be only fortuitous. The calculations show that the stabilities of the enol on the ring carbonyl and the amido carbonyl are similar.

N-Ph-MA is an enol of amide both in the solid state and in CCl_4 and $CDCl_3$ solutions,[6a] but its deviation from the open-chain diester line in Figure 3a is not surprising. MA is a much stronger acid in solution (pK_a = 4.83 (H_2O), pK_a (DMSO) = 7.32)[15a] than the open-chain analogue dimethyl malonate (pK_a (DMSO) = 15.87),[15b] and this was ascribed to the intrinsically higher acidity of the (*E*)-conformation of the ester moieties in MA than of the (*Z*)-conformation in the open-chain ester.[15c,d] Recent calculations[16] indicate that in addition, the MA enolate is preferentially stabilized by anomeric effects[16a] and by strong charge-transfer delocalization and electrostatic attraction between the anionic C1 and C4.[16b] In the gas-phase, MA is indeed a stronger acid than dimethyl malonate, but the acidity of its 5-=C(OH)NHR (R = Ph, *i*-Pr) derivatives seems to be lower than expected. It is unclear yet if the acidity of MA or of its derivatives causes the discrepancy.

Structural Changes on Ionization. The changes of the bond lengths on ionization are accounted for by three effects: (a) the zwitterionic nature of the enols (cf. **2a**); (b) the =O···H−X hydrogen bonding in the enols, which is stronger for X = O than for X = N; and (c) the negative charge delocalization in the anion shown by the valence bond structures **3**−**6** for the β-dicarbonyl-substituted systems as discussed below.

The largest change is the shortening of the C−O(H) bond length, accounted for by the classical enolate structure **4** displaying a C=O double bond for the same reason, since hybrids **4**−**6** have a single C_α−C_β bond. The negative charge delocalization into the two EWG−C=O groups should shorten the C−EWGs and elongate the C=O bonds. This is observed for the bonds to and in the C=O cis to the RNH group (cf. structure **5**). However, the opposite effect is shown for the C=O group cis to the enolic oxygen despite the suggested contribution of hybrid **6**.

We ascribe this apparent discrepancy to the loss of the O−H··O= hydrogen bond on ionization. The hydrogen bonded C=O to the O−H in the enol is always longer than the bond of the C=O hydrogen bonded to the N−H group. Only the former bond is lost on ionization with a consequent C=O shortening.

The appreciable elongation of the C_α−N bond is ascribed to the loss of its partial double-bond character in the enol (cf. **2a**) on ionization when the C_α−O bond acquires a negative charge.

---

(15) (a) Arnett, E. M.; Harrelson, J. A., Jr. *J. Am. Chem. Soc.* **1987**, *109*, 809. (b) Arnett, E. M.; Maroldo, S. L.; Schilling, S. L.; Harrelson, J. A. *J. Am. Chem. Soc.* **1984**, *106*, 6759. (c) Wang, X.; Houk, K. N. *J. Am. Chem. Soc.* **1988**, *110*, 1870. (d) Wiberg, K. B.; Laidig, K. E. *J. Am. Chem. Soc.* **1988**, *110*, 1872.

(16) (a) Byun, K.; Mo, Y.; Gao, J. *J. Am. Chem. Soc.* **2001**, *123*, 3794. (b) Lee, I.; Han, I. S.; Kim, C. K.; Lee, H. W. *Bull. Korean. Chem. Soc.* **2003**, *24*, 1141. (c) Nakamura, S.; Hirao, H.; Ohwada, T. *J. Org. Chem.* **2004**, *69*, 4309.

The loss of the zwitterionic character of the enol on ionization affects other bond lengths. As expected, the effect is more pronounced on C_α and the changes are the largest for bonds of the C_α-electron-donating groups. Smaller changes are observed at the $C_\beta(EWG)_2$ moiety, which is negatively charged in both the enol and the anion.

That the $C_\beta{-}CO_2R$ bond for the CO_2R group cis to the OH is elongated rather than contracted suggests a less negative charge delocalization to its C═O group in the anion than in **2a**. In the enol, the differences between the two C_β−EWG bonds are small and nonsystematic. In the anion, the significantly longer bond to the C═O group cis to the N−H than to the other C═O is ascribed to the loss of only the hydrogen bond to the latter.

Similar trends occur on ionization of the cyanoesters, except for almost no effect on the bond to the CN group cis to the N−H group. Since this group does not form intramolecular hydrogen bonds, the change enol → anion apparently does not cause an extensive delocalization. Most of the delocalization is by the C═O group with a consequent shortening of the C_β−C(═O) and lengthening of the C═O bonds, due to compensation of lengthening due to delocalization and shortening due to the hydrogen bond loss.

Acidity−K_{enol} Relationships. The effect of Y and Y′ on K_{enol} is due to substantial stabilizing effects on the enols and a substantial destabilizing effect on the amide.[6a,b,17a] The same applies also for the systems studied in the present work.[17b] In contrast, only the negative-charge-delocalizing ability of Y and Y′ should be dominant in determining the acidities ($\Delta G°_{acid}$) of our compounds. Consequently, we expect an increase in the K_{enol} values with more EWGs Y,Y′ as deduced from the contribution of hybrid **2a** to the stability of the enol. We therefore searched for $\Delta G°_{AE}$ vs $\Delta G°_{acid}$ correlation. Indeed the $\Delta G°_{AE}$ vs the observed $\Delta G°_{acid}$ plots are nearly linear for the *N*-Ph and *N*-Pr-*i* series (Figure 10). This linearity is a consequence of the linearity of $\Delta G°_{acid}$ values of the amides and their enols. Although the linearity suggests that the K_{enol} values can be roughly estimated within a series from the $\Delta G°_{acid}$ values, this prediction is limited. For example, *N*-Pr-*i* enols are significantly stronger acids than the *N*-Ph enols, but the K_{enol} values are much closer for the two series for the same YY′ and are not always lower for the *N*-Pr-*i* series. The highest experimental K_{enol} values in most solvents for the *N*-Pr-*i* than for the *N*-Ph series means that $(K^a_{amide}/K^a_{enol})_{N-Pr-i} > (K^a_{amide}/K^a_{enol})_{N-Ph}$. Since the calculated $(K^a_{enol})_{N-Ph}/(K^a_{enol})_{N-Pr-i} > 1$, $(K^a_{amide})_{N-Pr-i}/(K^a_{amide})_{N-Ph} > (K^a_{enol})_{N-Pr-i}/(K^a_{enol})_{N-Ph} < 1$. This conclusion is reasonable since the EWG phenyl will increase the acidity of both species, more than the electron-donating *i*-Pr group.

Of more practical interest would be the existence of a correlation between the $\Delta G°_{AE}$ values in solution and the gas-phase $\Delta G°_{acid}$ values. In solution the K_{enol} values display the following order for Y,Y′ in RNHCOCHYY′: $(CO_2Me)_2 < CO_2Me(CO_2CH_2CF_3) < (CO_2CH_2CF_3)_2 < CN(CO_2Me) < CN(CO_2CH_2CF_3) < CN(CO_2CH(CF_3)_2$. Experimental data on $(CN)_2$ are missing.[6b] The gas-phase $\Delta G°_{acid}$ values seem to follow this order. However, there are two problems with the experimental values.[6] First, the percentages of the enols decrease strongly with the increase in the solvent polarity. In $CDCl_3$, which is the optimal solvent for obtaining reliable K_{enol} values, the solubility of several of the compounds is small.[6] Moreover, since the K_{enol} values are determined by NMR, values >100 cannot be more accurately determined.

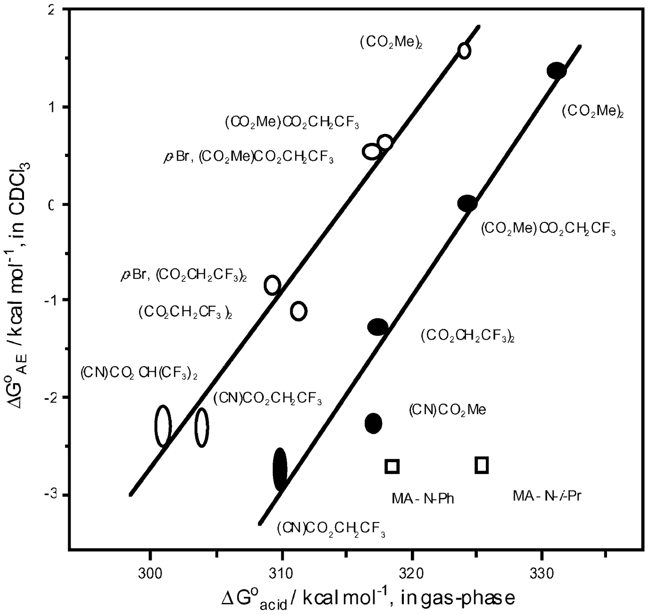

FIGURE 14. Plot of the experimental $\Delta G°_{AE}$ values in $CDCl_3$ against the experimental gas-phase $\Delta G°_{acid}$ values for the same species. Open circles, *N*-Ph systems. Slope = 0.182; $R^2 = 0.969$. Black circles: *N*-Pr-*i* systems. Slope = 0.203; $R^2 = 0.943$. Elipsoid points are for systems with $K_{enol} > 100$.

The correlation was tried for 14 systems, five of which with $K_{enol} > 50$. Figure 14 shows two reasonable linear correlations, one each for the *N*-Ph and *N*-Pr-*i* series, as in Figure 10, with the points for the MA-derivatives above these lines. The linearity suggests that, in solution, too, the $\Delta G°_{acid}$ values of the amides and their enols are linearly correlated.

The slopes of Figures 14 of 0.17−0.21 indicate a much higher sensitivity of the gas-phase acidity to the substituents than the $\Delta G°_{AE}$ values.

Within the limitations mentioned above, the plots in Figure 14 can serve as a successful guide for estimating K_{enol} values in solution from the gas-phase data for the limited series studied.

Calculated vs Observed Acidities. Figure 6a, which demonstrates the perfect linearity between the calculated and observed $\Delta G°_{acid}(CH_2YY')$ for the open-chain systems, the similarity of Figures 3 and 7, and the close and parallel observed and calculated plots of the acidities of the *N*-Ph vs the *N*-Pr-*i* series (Figure 1) give confidence to the quality of the calculations and to the nature of the ionized species. The corresponding calculated $\Delta G°_{acid}$ vs observed $\Delta G°_{acid}$ plot for the enols is similarly linear with the four cyclic compounds either on the line or close to it. Consistently, $\Delta G°_{acid}$ (calcd) > $\Delta G°_{acid}$ (obsd). The difference is the lowest for the YY′ = $(CO_2Me)_2$ derivative (4.5 kcal/mol), and since the slope of Figure 6 is 1.13, the differences between the observed and calculated values increase down the line, reaching a maximum (7.6 kcal/mol) for the strongest acid with YY′ = $(CN)CO_2CH(CF_3)_2$.

---

(17) (a) Rappoport, Z.; Lei, Y. X.; Yamataka, H. *Helv. Chim. Acta* **2001**, *84*, 1408. (b) Mishima, M.; Rappoport, Z. Unpublished results.

We ascribe the discrepancy between the observed and calculated values to the level of the calculations. Indeed, for Meldrum's acid where our $\Delta G°_{acid} = 324.9$ kcal/mol is the first one known in the gas phase, there are calculations at various levels.[16] Our values at B3LYP/6-31+G* and B3LYP/6-311+G** are 320.9 and 321.4 kcal/mol, respectively. Similar values (321.1 and 321.5) and 322.7 at B3LYP/6-311++G(2df,2p) were calculated by Lee and co-workers.[16b] However, at GB(+)(MP2)[16b] and B3LYP/Aug-cc-pVDZ,[16a] the value is 325.1 kcal/mol. Consequently, a very high-level calculation is required to reproduce the experimental value, and the convergence to the experimental value is lower at our level of calculation.

The dimedone value, which at G3(+)(MP2) is 328.5 kcal/mol,[17b] is still 2.6 kcal/mol lower than the NIST value of 331.2 kcal/mol.[10] Our calculated values for CH_2Y_2 (Y = COMe, CN) slightly reduce the gap with the experiment on increasing the level of calculations similarly to the MA value. Since the B3LYP/6-31+G* values for all the carbon acids CH_2YY' show approximately the same gap, we believe that this gap reflects the insufficient level of the calculation. The conclusion applies also for the discrepancy between the measured and calculated values for the trisubstituted methanes.

The calculated vs observed $\Delta G°_{acid}$ plots for the *N*-Pr-*i* systems (Figure 4) display similar linearities when calculated either for the enols or for the amides, disregarding the deviation of the $(CN)_2$ compound from the enol line. This prevents an unequivocal decision concerning the structure of the neutral species in the gas phase. Whereas the $(CO_2Me)_2$ and $(CO_2Me)CO_2CH_2CF_3$ derivatives are amides in the solid state and the other compounds are enols,[6c] the experimental and B3LYP/6-31+G* $\Delta G°_{acid}$ values differ to the same extent when calculated for the enol and the amide for the $(CO_2Me)_2$ system but are 1.2−2.2 kcal/mol closer when calculated for the enol than for the amide in the $(CO_2Me)CO_2CH_2CF_3$ derivatives. This difference will still lead to approximate linearity even if the neutral species in the gas phase for these two compounds differs from those for the other compounds. We believe that the compounds ionize as the enols since the values calculated for the enols are always closer to the experimental values than those calculated for the amides. The averages of the $\Delta G°_{acid}$ (obsd − calcd) are 3.3 ± 0.6 kcal/mol for the enols ($(CN)_2$ excluded) and 6.1 ± 1.0 kcal/mol for the amides. Moreover, the value for the $(CO_2Me)_2$ compounds at the higher B3LYP/6-31++G** level is 2.8 kcal/mol higher than for the amide and almost match the experimental value.

Similar plots for the *N*-Ph series (Figure 5) show again stronger calculated acidities for the amides, with larger differences than for the *i*-Pr systems. The plot for the enols shows significantly better linearity than that calculated for the amides, especially if the cyclic systems are also included. The difference between the observed and calculated $\Delta G°_{acid}$ values for the enols of 4.2 ± 0.6 kcal/mol (10.1 for the $(CN)_2$ are significantly smaller than those for the amides (9.2 ± 0.9 kcal/mol; $(CN)_2 = 6.4$ kcal/mol).

The plots of the calculated $\Delta G°_{acid}$ values for the *N*-Ph and *N*-Pr-*i* enols vs the $\Delta G°_{acid}$ values for CH_2YY' (Figure 7) are not expected to be linear for the whole series (a) since the CH_2YY' enolize from carbon and most of the enols from the oxygen and (b) due to additional electronic and steric effects in the N-substituted series. The small linear segments for each subfamily demonstrate that the acidities change more in the CH_2YY' series than in the more crowded systems.

Experimental Section

Materials. The enols, amides, and malonic acid derivatives were available from previous studies.[6b−e]

Gas-Phase Acidity Measurement. The gas-phase acidity measurements were performed on an Extrel FTMS 2001 Fourier transform mass spectrometer. Most of the experimental techniques used for the measurements of the equilibrium constants of the reversible proton-transfer reactions are the same as those given earlier.[9] Equations 5−8 describe the sequence of reactions that occurs in a typical experiment where AH and A_oH are the measured acid and the reference acid, respectively.

$$CH_3ONO + e^- \rightarrow CH_3O^- + NO \quad (5)$$

$$CH_3O^- + A_oH \rightarrow A_o^- + CH_3OH \quad (6)$$

$$CH_3O^- + AH \rightarrow A^- + CH_3OH \quad (7)$$

$$A^- + A_oH \rightleftharpoons A_o^- + AH \quad (8)$$

An experiment is initiated by a 5 ms pulse of a low-energy electron beam (0.3−0.5 eV) through the ICR cell. The electrons are captured by methyl nitrite at a partial pressure of 1.2×10^{-7} Torr, and CH_3O^- is produced. The acids AH and A_oH react with CH_3O^- to yield M − 1 negative ions. The partial pressure of the enols were maintained at lower than 4×10^{-7} Torr. The proton-transfer equilibrium was achieved within 10−200 s of initiation of the reaction (depending on the pressure of neutrals), and the equilibrium constant K for reaction 8 was evaluated from the expression $K = [A^-][A_oH]/[A_o][AH]$. The relative abundances of ions A^- and A_o^- were determined by the relative intensities of ICR mass spectra signals when the equilibrium was attained. For some cases the time for the establishment of equilibrium was over 200 s. The pressures of the neutral reactants were measured by means of a Bayard−Alpert-type ionization gauge applying appropriate correction factors to correct the gauge readings for the different ionization cross sections of various compounds.[18] Each experiment was performed at several ratios of the partial pressures and at different overall pressures. The proton-transfer reactions were examined by ion-eject experiments using the SWIFT technique.[19] In some cases, after an ion was ejected, the ratio of two ions at equilibrium did not give the same value as that obtained without ion ejection. This is probably due to competition of proton transfer with ion loss because the proton-transfer reaction was too slow. The arithmetic means of the values of K were used to calculate $\Delta G°$ at 323 K, the average uncertainty being ±0.2 kcal/mol in most of these cases. Each value was measured with two reference acids. The gas-phase acidity values for the reference compounds were taken from the literature.[10] Most of the compounds investigated in this study are low-volatility solids. The solid sample direct-inlet systems and all vacuum chamber systems were kept at 80−100 °C. The ionization gauge shielded from strong magnetic field by use of a magnetic shield foil (Fe−Ni alloy) was directly set at the main vacuum chamber to read the precise pressure in the ICR cell, because the ionization gauge that was originally set at the small pipe connected with the main chamber gave a lower

---

[18] (a) Bartmess, J. E.; Georgiadis, R. M. *Vacuum* **1983**, *33*, 149. (b) Miller, K. J. *J. Am. Chem. Soc.* **1990**, *112*, 8533.

[19] Marshall, A. G.; Wang, T.-C. L.: Ricca, T. L. *J. Am. Chem. Soc.* **1985**, *107*, 7983. Cody, R. B. *Analysis* **1990**, *16*, 30. Guan, S.; Marshall, A. G. *Int. J. Mass Spectrom. Ion Process* **1997**, *157/158*, 5.

reading of the pressure when low-volatility compounds were introduced into the cell through a solid probe. In addition, the pumping speed was also reduced by use of the gate valve, which was set between the main chamber and a turbomolecular pump. The background pressure was kept at less than 10^{-8} Torr.

Calculations. Conformational searches were carried out using Spartan ‘02 program (Wavefunction, Inc.), and several conformers that have the lowest energy were further optimized at the RHF/3-21G* level of theory to search the lowest energy conformer (global minimum). Finally, the geometries were fully optimized at the B3LYP/6-31+G* level of theory with normal convergence using the Gaussian 98 program.[20] Vibrational normal-mode analyses were performed at the same level to ensure that each optimized structure was a true minimum on the potential energy surface and to calculate the thermal correction needed to obtain the Gibbs free energies. The zero-point energies used for the thermal correction were unscaled. Several systems were calculated further at the higher B3LYP/6-311+G*//B3LYP/6-311+G* and B3LYP/6-311+G**//B3LYP/6-311+G** levels.

Acknowledgment. This paper is dedicated to Professor H. Schwarz on the occasion of his 60th birthday. We are indebted to the Ministry of Education, Culture, Sport, Science and Technology, Japan, and the Israel Science Foundation for support, to Professor Ilmar Koppel for supplying several reference acids, to Professor Leo Radom for discussions, and to Dr. Jayanta Mukhopadhyaya for a few of the cyclic enols.

Supporting Information Available: Table S1−S5, including bond lengths for various CH_2YY' systems, their enols and amides, the natural charges in these species, and dipole moments of the enols and amides, and Figures S1−S3 giving plots of calculated vs observed $\Delta G°_{acid}$ values and of ΔG_{AE} vs $\Delta G°_{acid}$ values and the calculated structures for most of the systems studied. This material is available free of charge via the Internet at http://pubs.acs.org.

JO040196B

---

(20) Frisch, M. J.; Trucks, G. W.; Schlegel, H. B.; Scuseria, G. E.; Robb, M. A.; Cheeseman, J. R.; Zakrzewski, V. G.; Montgomery, J. A., Jr.; Stratmann, R. E.; Burant, J. C.; Dapprich, S.; Millam, J. M.; Daniels, A. D.; Kudin, K. N.; Strain, M. C.; Farkas, O.; Tomasi, J.; Barone, V.; Cossi, M.; Cammi, R.; Mennucci, B.; Pomelli, C.; Adamo, C.; Clifford, S.; Ochterski, J.; Petersson, G. A.; Ayala, P. Y.; Cui, Q.; Morokuma, K.; Malick, D. K.; Rabuck, A. D.; Raghavachari, K.; Foresman, J. B.; Cioslowski, J.; Ortiz, J. V.; Stefanov, B. B.; Liu, G.; Liashenko, A.; Piskorz, P.; Komaromi, I.; Gomperts, R.; Martin, R. L.; Fox, D. J.; Keith, T.; Al-Laham, M. A.; Peng, C. Y.; Nanayakkara, A.; Gonzalez, C.; Challacombe, M.; Gill, P. M. W.; Johnson, B. G.; Chen, W.; Wong, M. W.; Andres, J. L.; Head-Gordon, M.; Replogle, E. S.; Pople, J. A. *Gaussian 98*, revision A.5; Gaussian, Inc.: Pittsburgh, PA, 1998.